# High-performance electrochromic devices based on poly[Ni(*salen*)]-type polymer films

Marta Nunes,[a] Mariana Araújo,[a] Joana Fonseca,[b] Cosme Moura,[c] Robert Hillman[d] and Cristina Freire[a*]

[a] REQUIMTE/LAQV, Departamento de Química e Bioquímica, Faculdade de Ciências, Universidade do Porto, 4169-007 Porto, Portugal

[b] CeNTI, Rua Fernando Mesquita, 2785, 4760-034 Vila Nova de Famalicão, Portugal

[c] CIQ, Departamento de Química e Bioquímica, Faculdade de Ciências, Universidade do Porto, 4169-007 Porto, Portugal

[d] Department of Chemistry, University of Leicester, Leicester LE1 7 RH, UK

*Corresponding author: Dr. Cristina Freire; e-mail: acfreire@fc.up.pt
Tel.: +351 22 04020590; Fax: +351 22 0402 695.

**ABSTRACT**

We report the application of two poly[Ni(*salen*)]-type electroactive polymer films as new electrochromic materials. The two films, poly[Ni(3-Mesalen)] (poly[1]) and poly[Ni(3-MesaltMe)] (poly[2]), were successfully electrodeposited onto ITO/PET flexible substrates and their voltammetric characterization revealed that poly[1] showed similar redox profiles in $LiClO_4/CH_3CN$ and $LiClO_4$/ propylene carbonate (PC), while poly[2] showed solvent dependent electrochemical responses. Both films showed multielectrochromic behaviour, exhibiting yellow, green and russet colours according to their oxidation state, and promising electrochromic properties and high electrochemical stability in $LiClO_4$/PC supporting electrolyte. In particular, poly[1] exhibited a very good electrochemical stability, changing colour between yellow and green ($\lambda$ = 750 nm) during 9000 redox cycles, with a charge loss of 34.3 %, an optical contrast of $\Delta T$ = 26.2 % and an optical density of $\Delta$OD = 0.49, with a colouration efficiency of $\eta$ = 75.55 $cm^2\ C^{-1}$. On the other hand, poly[2] showed good optical contrast for the colour change from green to russet ($\Delta T$ = 58.5 %), although with moderate electrochemical stability. Finally, poly[1] was used to fabricate a solid state electrochromic device using lateral configuration with two figures of merit: a simple shape (typology 1) and a butterfly shape (typology 2); typology 1 showed the best performance with optical contrast $\Delta T$ = 88.7 % (at $\lambda$ = 750 nm), colouration efficiency $\eta$ = 130.4 $cm^2\ C^{-1}$ and charge loss of 37.0 % upon 3000 redox cycles.

*Keywords:* Conducting polymers, Metal *salen* complexes, Spectroelectrochemistry, Electrochromism, Solid-state electrochromic cell.

## 1. INTRODUCTION

The focus on electrochromic (EC) materials started after the pioneering work done by Deb[1] in 1969 on electrochromism, which occurs when electroactive species exhibit reversible change or bleaching of colour, upon their electrochemical oxidation / reduction.[2,3,4] Currently, EC materials are mainly applied in smart windows for green architecture[5] and in anti-glare rear view mirrors.[6] Other proposed applications are in displays of portable and flexible electronic devices, including smart cards, re-usable price labels and electronic papers,[7,8,9] protective eyewear[10] and in textiles for adaptative camouflage or simply for fashion.[11]

To take advantage of the special properties of the EC materials in these practical and commercial applications, it is necessary their suitable integration into solid-state electrochromic cells (electrochromic devices, ECDs). The prototype ECDs are generally fabricated using optically-transparent electrodes, in a "sandwich"[12] or lateral[13] configurations, and consist of two electrodes (in which at least one is composed of an EC material), separated or covered by a layer of electrolyte.[6] With the application of an appropriate electrical potential, the colour change occurs as a result of the charge / discharge of the cell.[14,15]

Among the several known EC materials (e.g. *Prussian Blue*,[16] $WO_3$[17] and viologens[18]), conducting polymers (CPs)[19] have attracted particular attention due to their outstanding colouration efficiency, fast switching times, multichromism, high optical and electrochemical stability, thin film mechanical flexibility and cost effectiveness.[20,21,22] In fact, several works have been reported the EC behaviour of the polypyrrole,[23,24,25] polyaniline (PANI),[26] polythiophene[27,28] and their derivatives, as well as the fabrication of efficient complementary ECDs comprising CPs (e.g. polythiophene-derivatives@PANI[29,30] and polypyrrole@polythiophene-derivatives[31]). Typically, the

electric conductivity of these CPs are very high, but can be limited by the existence of structural defects which may interrupt the mobility of charge carriers. A new class of conducting polymers can be designed by incorporation of transition metals as functional groups or as units within the polymer backbone. The latter can be achieved by the preparation of poly[M(*salen*)]-type films (M = transition metal).[32]

The electroactive poly[M(*salen*)] metallo-polymers films are formed through the oxidative polymerization of transition metal complexes with *salen*-type ligands onto the electrode surface,[33] and exhibit poly(phenylene)-like properties, with the transition cations acting as a bridge between the phenyl rings.[34] Their potential application as EC materials have been explored by Freire's group.[35,36] The colorimetric properties of polymers based on *salen*-type complexes of Cu(II), Ni(II) and Pd(II) deposited over transparent flexible electrodes of polyethylene terephthalate coated with indium tin oxide (ITO/PET) were first studied by Pinheiro *et al.*,[35] using the CIELAB coordinates and spectroelectrochemical studies. More recently, Branco *et al.* [36] studied other series of [M(*salen*)]-derived electroactive films and selected materials were chosen to build homemade ECDs, whose preliminary performance was also assessed. The reported results addressed some promising EC properties for the poly[M(*salen*)] films in terms of colour changes and optical contrasts, but they showed moderate electrochemical stabilities which is one of the drawbacks for technological applications. Nevertheless, the results showed that the synthetic versatility of the metal *salen* complexes (by the introduction of different substituents into the *salen* skeleton or by using different metal centres) allowed fine tuning of the final EC features of the resulting polymeric systems, providing important guidelines for film molecular design optimization.

These observations motivated us to more detailed studies in order to achieve other poly[M(*salen*)]-type films with improved EC performance and electrochemical stability.

Consequently, in this paper we report the preparation and study of two novel electrochromic systems based on the electroactive polymers: poly[Ni(3-Mesalen)], *N*,*N'*-bis(3-methylsalicylideneiminate) nickel(II) (poly[1]), and poly[Ni(3-MesaltMe)], *N*,*N'*-2,3-dimethylbutane-2,3-dyil-bis(3-methylsalicylideneiminate) nickel(II) (poly[2]); both *salen* ligands have a methyl group in the 3-position of each salicylaldehyde moiety and differ on the absence/presence of methyl substituents in the imine bridge, respectively. For the first time, the influence of two electrolyte solutions – $LiClO_4/CH_3CN$ or $LiClO_4$/PC – on the redox and optical properties of the films was evaluated. The studies allowed the full evaluation of EC properties (switching times, optical contrasts and densities, colouration efficiencies and electrochemical stabilities), and were used as guidance to choose poly[1] as the polymeric film with the best EC properties for ECD fabrication with flexible substrates, using a lateral configuration with two figures of merit: simple lateral assemblage and butterfly shape. The former EC device showed the best promising EC performance and electrochemical stability: optical contrast $\Delta T$ = 88.7 % ($\lambda$ = 750 nm), colouration efficiency $\eta$ = 130.4 $cm^2\ C^{-1}$ and charge loss of 37.0 % upon 3000 redox cycles. This work corresponds to a step forward in the design of EC materials and device fabrication based in poly[M(*salen*)] films, since poly[1] surpassed all the previous EC metallopolymers analogues[35,36] and are competitive with other EC materials[20,37,38] for electronic devices, smart cards or labels.

## 2. EXPERIMENTAL

### 2.1 Materials and instrumentation

The complexes *N*,*N'*-bis(3-methylsalicylideneiminate) nickel(II), [Ni(3-Mesalen)] [1], and *N*,*N'*-2,3-dimethylbutane-2,3-dyil-bis(3-methylsalicylideneiminate) nickel(II), [Ni(3-MesaltMe)] [2] and respective *salen* ligands were prepared by methods described

in the literature.[39] Acetonitrile and propylene carbonate (PC) (Romil, pro analysis grade), $LiClO_4$ (Aldrich, purity 99 %) and poly(methylmethacrylate) (PMMA, Aldrich) were used as received.

The X-ray Photoelectron Spectroscopy (XPS) measurements were performed at CEMUP (Porto, Portugal), in a VG Scientific ESCALAB 200A spectrometer using non-monochromatised Al Kα radiation (1486.6 eV). The XPS spectra were deconvoluted with the XPSPEAK 4.1 software, using a non-linear least squares fitting routine after a Shirley-type background subtraction. To correct possible deviations caused by sample charging, the C 1s band at 284.6 eV was taken as internal standard. The surface atom percentages were calculated from the corresponding peak areas, using sensitivity factors provided by the manufacturer.

Scanning Electron Microscopy / Energy-dispersive X-ray Spectroscopy (SEM / EDS) analyses were performed at CEMUP (Porto, Portugal) in a high resolution environmental scanning electron microscope FEI Quanta 400 FEG ESEM, attached to an EDAX Genesis X4M X-ray spectrometer. The micrographs were obtained in secondary and backscattered electron modes.

Electrochemical studies were performed using an Autolab PGSTAT 30 potentiostat/galvanostat (EcoChimie B.V.), controlled by a GPES software. Studies in solution were performed on a three-electrode and single or separate compartment cells, enclosed in a grounded Faraday cage, using an Ag/AgCl (NaCl / 1.0 mol $dm^{-3}$) electrode (Metrohm ref. 6.0724.140) as the reference electrode, a Pt wire or a Pt grid (in the case of separate compartment cell) as the counter electrode and poly(ethylene terephthalate) (PET) coated with indium tin oxide (ITO) (ITO/PET) (Aldrich, resistivity of 60 Ω $sq^{-1}$) as the working electrode. Coulometric studies used a Pt disk working electrode (area 0.0314 $cm^2$, BAS), which was previously polished with aluminium oxide of particle size

0.3 μm (Buehler) on a microcloth polishing pad (Buehler), then washed with ultra-pure water (resistivity 18.2 MΩ cm at 25°C, Millipore) and $CH_3CN$.

The spectroelectrochemical studies were performed *in situ* using an Agilent 8453 spectrophotometer (with diode array detection) coupled to the potentiostat/galvanostat. The experimental apparatus comprised a teflon cell with an Ag/AgCl (NaCl / 3.0 mol $dm^{-3}$) (Bio-Logic) reference electrode, a Pt grid counter electrode and ITO/PET (typical area 0.785 $cm^2$) as working electrode. Particularly, in the ECD monitoring, were used a Perkin Elmer Lambda 35 UV/Vis spectrometer, coupled to an Autolab PGSTAT 302N potentiostat/galvanostat (EcoChimie B.V.).

**2.2 Preparation and characterization of polymeric films**

The poly[Ni(*salen*)] films were deposited potentiodynamically from corresponding monomer solutions (1.0 mmol $dm^{-3}$ [Ni(*salen*)] in 0.1 mol $dm^{-3}$ $LiClO_4/CH_3CN$), by cycling the potential of the working electrode (ITO/PET 3.0 $cm^2$) between 0.0 and 1.3 V, at the scan rate of 0.02 V $s^{-1}$, during 10 cycles; other conditions are specified in the corresponding text and figure legends.

After film deposition, the modified electrodes were rinsed with $CH_3CN$, immersed in monomer-free 0.1 mol $dm^{-3}$ $LiClO_4/CH_3CN$ or $LiClO_4$/PC solutions and cycled voltammetrically in the potential ranges 0.0 – 1.3 V or 0.0 – 1.4 V, at 0.020 V $s^{-1}$. The electroactive surface coverage, $\Gamma$ / μmol $cm^{-2}$ of each film was determined by a coulometric assay,[32,40] using cyclic voltammograms obtained in monomer-free 0.1 mol $dm^{-3}$ $LiClO_4/CH_3CN$ solution at a scan rate $v$ = 0.01 V $s^{-1}$, to ensure complete film redox conversion. The doping level ($n$) values used for $\Gamma$ determination were calculated from comparison of coulometric data for films deposition and cycling in 0.1 mol $dm^{-3}$ $LiClO_4/CH_3CN$ solution with the Pt electrode, as described in literature,[32,40] considering

that the obtained *n*-values are valid for other electrode substrates; the *n*-values were found to be *n* = 0.69 and 0.08 for poly[1] and poly[2], respectively. Although the values are very different from each other, this is recognised behaviour for these systems and both values are in the range known for poly[M(*salen*)] films; [32,34] their difference cannot be rationalized in terms of monomer ligand structures, which are very similar. Consequently, the supramolecular film structure may have an important key role in the degree of film doping, that is usually difficult to anticipate and quantify.

The monitoring of the redox process by *in situ* UV-Vis spectroscopy was performed with films prepared with 5 electrodeposition cycles. The films were subsequently cycled five times between -0.1 and 1.3 V, at $v = 0.020$ V $s^{-1}$, using monomer-free $LiClO_4/CH_3CN$ or $LiClO_4$/PC 0.1 mol $dm^{-3}$ solutions. The UV-Vis spectra were acquired simultaneously at 0.5 s intervals, in the wavelength range of 315 - 1100 nm. The molar extinction coefficients, ε / $cm^{-1}$ $mol^{-1}$ $dm^3$, of all observed electronic bands were estimated using a combination of the Beer-Lambert and Faraday laws (Equation 1):[32,40,41]

$$Abs(\lambda) = \varepsilon\,(\lambda)\; Q / nFA \qquad (1)$$

where $Q$ is the charge (C), $n$ is the doping level, $F$ is the Faraday constant and $A$ the electrode area ($cm^2$).

Films for SEM/EDS and XPS analysis were prepared with 10 and 15 cycles and the reduced and oxidized states were achieved by the application of 0.0 or 1.3 V, during 300 s, in a monomer-free $LiClO_4/CH_3CN$ 0.1 mol $dm^{-3}$ solution, after the electrodeposition. For poly[1] were also studied by XPS reduced and oxidized films in $LiClO_4$/PC 0.1 mol $dm^{-3}$.

### 2.3 Electrochromic properties evaluation

The EC properties of the films were explored by a double potential step method (chronoamperometry) coupled with UV-Vis spectroscopy (chronoabsorptometry). The studies were performed in 0.1 mol $dm^{-3}$ $LiClO_4/CH_3CN$ or $LiClO_4$/PC solutions, considering two possible colour transitions: yellow ↔ green and green ↔ russet. In the double potential step experiment, the potential was set at the initial potential value (0.0 or 0.7 V, according to the colour change) for a period of time of 50 s and was stepped to a second potential (0.7, 1.3 or 1.15 V) for another period of 50 s, being after switched back to the initial potential. The simultaneous chronoabsorptometric measurements were performed at the fixed wavelengths of λ=510 nm (green ↔ russet) and λ=750 nm (yellow ↔ green), acquiring the UV-Vis spectra at intervals of 1 s, during 4 redox cycles. The films used in these studies were electrodeposited using 5 potentiodynamic cycles.

Electrochemical stability tests were performed by chronoamperometry, using the same experimental conditions, but over extended time intervals (400 – 9000 redox cycles, ca.11 hours – 11 days). The films used in these studies were prepared with 10 electrodeposition cycles.

The change of the optical density, ΔOD, (or optical absorbance change, ΔAbs), was estimated using the Equation 2:[15]

$$\Delta Abs\ (\lambda) = \Delta OD\ (\lambda) = \log\ (T_{red}(\lambda) / T_{ox}(\lambda)) \quad (2)$$

where $T_{red}$ and $T_{ox}$ are the transmittance values of the films in reduced and oxidized states, at a fixed wavelength (λ=510 or 750 nm).

The colouration efficiency, $\eta$, is defined as the change of the optical density, ΔOD, and it was estimated by considering the total charge passed during the potential pulse, per unit area, $Q_d$:[15,12]

$$\eta = \Delta OD / Q_d \quad (3)$$

## 2.4 Fabrication and characterization of electrochromic devices

ECDs were built using as EC material poly[1] films electrodeposited on flexible substrates of ITO/PET (4.5 × 3.0 $cm^2$). The devices were assembled in lateral configuration, with the electrodes side-by-side, in two different typologies: typology 1, with a simple shape, and typology 2, with a butterfly shape. Both electrodes are based on the same EC material and, in case of the device of typology 2, one of the electrodes corresponds to the butterfly inside area, while the other corresponds to the butterfly outside area.

Following film deposition, the ECDs were assembled by making a cut under the film and ITO surface, in order to define the limits of each electrode and prevent electrical contact between each part. The cut is a simple vertical line in case of ECD of typology 1 and corresponds to the butterfly shape for device of typology 2. Then, a layer of a PMMA-based electrolyte was deposited over both electrodes.

The poly[1] films were electrodeposited potentiodynamically in the potential range 0.3 to 1.5 V, at $\nu$ = 0.020 V $s^{-1}$, for 10 cycles and with slow stirring, in the two compartment cell. The electrolyte was a semi-solid polymeric electrolyte based on PMMA, prepared by a procedure adapted from literature.[42] Briefly, a mixture of PMMA (7 %), $LiClO_4$ (3 %), $CH_3CN$ (58 %) and PC (32 %) (% m/m) was stirred during about 20 hours, at room temperature, to yield a translucent and malleable gel. We note that the high viscosity of this type of electrolyte makes it impractical for conventional electrochemical cell configurations (see above), but its use was explored here in device configuration as a consequence of its relevance to practical applications.

The ECD of typology 1 were characterized by chronoamperometry, during 3000 redox cycles, applying potential pulses of 200 s, with potential alternating between -1.0 and 1.0 V (colour transition yellow ↔ green). During the first 1000 redox cycles, the

experiment was monitored by UV-Vis spectroscopy (chronoabsorptometry), at λ=750 nm. The ECD of typology 2 was also characterized by chronoamperometry, but applying potential pulses of 100 s, with potential alternating between -1.1 and -0.25 V (yellow ↔ green). Note that these potential values are, in reality, potential differences between the two electrodes; since there is no reference electrode, potential values are not directly placed on an absolute scale.

## 3. RESULTS AND DISCUSSION

### 3.1 Electrochemical preparation and characterization of polymeric films

The voltammetric responses obtained during the electropolymerization of both [Ni(*salen*)] complexes are depicted in Figure 1 and the peak potential values are summarized in Table S1, in Supporting Information (SI).

Figure 1

In the first anodic half-cycle, two peaks are observed at $E_{pa}$ = 0.87 and 1.08 V and one peak at $E_{pa}$ = 0.99 V for [Ni(3-Mesalen)] [1] and [Ni(3-MesaltMe)] [2] complexes, respectively, which are attributed to the oxidation of monomers, resulting in formation of oligomers/polymer in the vicinity of the working electrode surface.[32] In the reverse scan, two peaks are detected at $E_{pc}$ = 0.69 and 0.20 V for [Ni(3-Mesalen)] and one peak at $E_{pc}$ = 0.64 with a slight inflection at $E_{pc}$ = 0.50 V for [Ni(3-MesaltMe)], which correspond to the reduction of film deposited in the preceding anodic scan.[43,44] In the second and subsequent voltammetric cycles (5$^{th}$ cycle in Table S1), a new peak appears at $E_{pa} \approx 0.42$ V for the [Ni(3-Mesalen)] system which is assigned to polymer film oxidation deposited during the previous cycle(s);[43,44] in the reverse cathodic, the peaks at $E_{pc}$ = 0.64 and 0.22

V are due to the oligomers and polymer film reductions. In the case of [Ni(3-MesaltMe)], two new peaks appear during the second and subsequent scans ($5^{th}$ cycle in Table S1) at $E_{pa}$ = 0.59 and 0.68 V, due to polymer film oxidation and the peak attributed to the monomer oxidation shows now a slight inflexion at $E_{pa}$ = 1.17 V; the second and the following cathodic scans are significantly different from the $1^{st}$ one, showing three cathodic waves at $E_{pc}$ = 0.87 V (oligomers reduction) and $E_{pc}$= 0.58 and 0.45 V, due to polymer film reduction.

The growth of both polymers is proved by the increasing of current intensity of the peaks corresponding to the oxidation and reduction of film in consecutive cycles, and by the visual inspection of a green film deposited on the electrode surface at the end of the process.

The voltammetric responses of the as-prepared poly[1] and poly[2] films in the electrolyte solutions $LiClO_4/CH_3CN$ and $LiClO_4$/PC 0.1 mol $dm^{-3}$ are depicted in Figure 2 and, in Table S2, are summarized the potential peak values.

Figure 2

It is possible to identify two anodic peaks at $E_{pa}$ = 0.39-0.88 V and $E_{pa}$ = 0.94-1.29 V and two cathodic peaks at $E_{pc}$ = 0.17-0.41 V and $E_{pc}$ = 0.56-0.83 V. The results revealed that poly[1] film showed similar redox profiles either in $LiClO_4/CH_3CN$ or $LiClO_4$/PC electrolytes. In contrast, electrochemical responses of poly[2] obtained in $LiClO_4$/PC present greater peak separation (anodic peaks at more positive potentials and the cathodic peaks at less positive potentials) than those obtained in $LiClO_4/CH_3CN$. The different redox response of poly[2] in the two electrolyte solutions can be related with the monomer ligand structure; in the case of poly[2] the imine bridge presents four methyl groups,

which may have different conformations in the two used electrolyte solutions, leading to distinct supramolecular structures, that may induced different electrochemical responses.

We note additional anodic charge in the response to the first voltammetric cycle in background electrolyte. This is attributed to (irreversible) completion of the polymerization process for modest amounts of monomer and/or oligomer trapped within the film. In general, the voltammetric responses of polymeric films stabilised after 5 scans, which correspond to the typical "film conditioning".[43,45] The coulometric data revealed $\Gamma$ = 0.31 and 1.13 μmol $cm^{-2}$ for poly[1] and poly[2], respectively, suggesting greater polymerization efficiency for poly[2].

### 3.2 Compositional and morphological characterizations

Surface analysis of poly[Ni(*salen*)] films in reduced and oxidised states (at *E*=0.0 V and *E*=1.3 V) was performed by XPS. Surface atomic percentages and atomic ratios are summarised in Table 1 for poly[1] in $LiClO_4/CH_3CN$ and $LiClO_4$/PC and in Table S3 for poly[2] in $LiClO_4/CH_3CN$.

| Table 1 |
| --- |

For poly[1] and poly[2] reduced films in $LiClO_4/CH_3CN$, the XPS-derived atomic ratios N/Ni and O/Ni are slightly higher than those expected, based on the Ni:*salen* stoichiometric ratio, N/Ni = O/N = 2. Combined with the appearance of Cl, this indicates the presence of $ClO_4^-$ and/or $CH_3CN$ at low levels, as result of the supporting electrolyte trapping in polymeric matrixes during the deposition or cycling processes.[32] In comparison, the oxidized poly[1] and poly[2] films showed higher N/Ni, O/Ni and Cl/Ni atomic ratios. This significant increase, (higher for O/Ni and Cl/Ni ratios) is explained by

the presence $ClO_4^-$/$CH_3CN$ inside the films, due to the charge compensation/solvation during the films oxidation, as observed previously for similar systems[32] (deconvoluted XPS spectra in O1s region for reduced and oxidized poly[1] in Figure S1 in SI). This assumption is supported by the increase of the Cl/O ratio in a proportion of ca. 1:4 (in agreement with $ClO_4^-$ composition) from the reduced to the oxidized films. In $LiClO_4$/PC, poly[1] film showed similar changes in atomic ratios on going from the reduced to the oxidised state, which can be interpreted as in $LiClO_4$/$CH_3CN$ electrolyte solution. Furthermore, it is worth to mention, that there is a larger increase in O/Ni and Cl/Ni ratios, from the reduced to the oxidized state, in $LiClO_4$/$CH_3CN$ (increase of 79.7 %) than in $LiClO_4$/PC (increase of 36.4 %), suggesting a higher degree of $ClO_4^-$ ingress during film oxidation in the former electrolyte solution. Another interesting aspect, when compared poly[1] and poly[2] films in $LiClO_4$/$CH_3CN$ electrolyte solution, is that both O/Ni and Cl/Ni ratios are lower in the reduced state and higher in the oxidized state of poly[1]. This indicates a lower % of $Li^+ClO_4^-$ entrapped within poly[1] film matrix relatively to poly[2] in the reduced state, but a higher % of $ClO_4^-$ occluded in the oxidized state; this maybe to some extent a consequence of the higher n-doping value of poly[1] ($n$=0.69) compared to poly[2] ($n$=0.08). In XPS analysis of both films it was also detected $Li^+$ (from $Li^+ClO_4^-$ ion pairs) at very low levels, 0.26 % or non-detected for poly[1] in the reduced and oxidized states, respectively, whereas for poly[2] the Li% is 1.55 and 0.31 for the reduced and oxidized states, respectively; this suggests that the oxidation charge compensation in this polymer film is to a certain degree attained by $Li^+$ egress. However, due to the low sensitivity of XPS instrumentation for Li element, the small Li % have high inaccuracy, and consequently were not considered in the calculation of the values presented in Tables 1 and S3. Furthermore, it should be mention that the XPS results refer to typically 4-5 nm from the total film thickness.

In Figure 3 are depicted SEM micrographs and EDS spectra for poly[1] films on reduced and oxidized states; SEM images of the surface of poly[2] films (not shown) reveal a similar morphology.

Figure 3

The films consisted of a continuous layer (Z2), on top of which there are irregular fragments of higher dimensions (Z1). The EDS spectra showed that, in the Z1 regions, the Ni element (from polymeric film) is present in higher quantity than In (from substrate), while, in Z2 regions, the In content increases considerably in comparison to Ni. These results indicate that the film surface and thickness are not uniform. The EDS spectra revealed yet a higher Cl content in oxidized film (in agreement with XPS results) and the respective micrograph showed a bulkier film, possibly due to the ingress of supporting electrolyte into the polymeric matrix.

### 3.3 UV-Vis spectroscopy *in situ*

In Figures 4 (a) and (b) are depicted the absolute UV-Vis spectra acquired during the oxidations of poly[1] films in $LiClO_4/CH_3CN$ and $LiClO_4$/PC 0.1 mol $dm^{-3}$, respectively; the equivalent spectra for poly[2] are depicted in Figure S2 (a) and (b), SI; the spectra obtained during films reduction showed an inverse behaviour and were omitted for simplicity.

Figure 4

The poly[1] spectra show four bands in both electrolytes. For poly[2], four electronic bands are observed in $LiClO_4/CH_3CN$, whereas in $LiClO_4$/PC five bands are observed. The bands show different dependences on applied potential and, so, their intricate behaviours are most readily appreciated by depicting the difference spectra, using the responses at selected potentials as reference points, Figures S3 and S4 for poly[1] and poly[2], respectively. The absorbance vs. potential profiles (*Abs* vs. *E*) for wavelengths of detected bands (Figure 4 (a') and (b') and Figure S2 (a') and (b')), allowed the identification of three main band profiles with increasing potential in both electrolytes: (i) bands at λ=327 and 330 nm for poly[1] and poly[2], respectively, showed a monotonically intensity decrease during the positive half cycle, (ii) bands in the range λ=402-415 nm and λ=843->950 nm showed intensity increase until *E* = 0.8-0.9 V and thereafter decreased until the end of the positive half cycle, and (iii) bands in the range λ=510-525 nm for poly [1] and poly[2] and at λ=639 nm (poly[2] in $LiClO_4$/PC), showed monotonically intensity increase from *E* = 0.8-0.9 V until the end of the positive half scan. Curiously, the maximum intensity of the electronic bands at λ=510 nm for poly[1] and at λ=520/525 nm for poly[2], is significantly lower in $LiClO_4$/PC than in $LiClO_4/CH_3CN$.

Table 2 summarizes data for the observed electronic bands for both polymers in the two electrolytes: $\lambda_{max}$ (nm), molar extinction coefficients, ε, (estimated from Equation 1, through the slopes of *Abs* vs. *Q* plots, Figure S5 in SI) and *E* (eV).

Table 2

Both polymers showed similar energy values for all the electronic bands as a consequence of their similar monomer structures; furthermore, the electronic band

energies for each polymer film are also similar for the two electrolytes, indicating that the polymer structures are comparable in both electrolytes.

The results also revealed that, for each film, all the electronic bands have similar ε-values in $LiClO_4/CH_3CN$ and $LiClO_4$/PC electrolytes, with the exception of the band at λ=510 nm for poly[1] and λ=520 / 525 nm for poly[2], which ε-values are lower in $LiClO_4$/PC than in $LiClO_4/CH_3CN$ (for poly[1], the ε-value decreased from $19.7 \times 10^3$ to $13.6 \times 10^3$ $cm^{-1}$ $mol^{-1}$ $dm^3$).

For both polymers, all the electronic bands ε-values are typical of electronic transitions between states with large contribution from ligand orbitals, which is consistent with the assertion of ligand-based film oxidation.[32,40,46] Consequently, the electronic bands can be assigned according to the polaronic model.[32,40] The electronic bands with the same *Abs* vs. *E* (or *Q*) profiles can be associated with the same charge carriers, whereby the following band assignment is proposed: (i) the electronic bands at λ=327 / 330 nm (3.79 eV and 3.76 eV) are assigned to the intervalence band (band gap), since they represent the largest energy transition and decrease in intensity upon polymer oxidation; (ii) the bands at λ=402 /415 nm (3.09 eV and 2.99 eV) are attributed to the transition between the valence band and the antibonding polaron level and (iii) the bands at λ=843 nm and λ>950 nm (1.47 and 1.31 eV) are ascribed to the transition from the bonding to the antibonding polaron levels (or from the valence band to the bonding polaron level). The other band predicted by the polaronic model was estimated to be at λ=766 and λ=738 nm (1.62 and 1.68 eV) for poly[1] and poly[2], respectively; these would most likely be overlapped with the bands at λ=843 and λ>950 nm and thus not separately observed. Lastly, the very intense bands at λ=510 nm (2.43 eV), λ=520 / 525 nm (2.39 / 2.36 eV) and λ=639 nm (1.94 eV) (for poly[2] in $LiClO_4$/PC) showed different *Abs* vs. *E* profiles and consequently cannot be assigned to the same charge carriers and

explained by the polaronic model. Since the band absorbance starts to increase at high oxidation potentials and their ε-values depend on the solvent ($CH_3CN$ vs. PC), unlike the other observed electronic transitions, they are assigned to charge transfer transitions between the metal and the oxidised ligand.[32,40]

### 3.4 Electrochromic properties evaluation

The visual inspection of both poly[Ni(*salen*)] films during redox cycling allowed the observation of their colour changes. Figure 5 shows photographic images of the film distinct colours as a function of the potential: in the reduced state (0.0 V) the films are yellow, switch to green at 0.7 V, and then to russet (reddish-brown) at 1.3 V.

Figure 5

To explore the potential application of both films as EC materials, a square-wave potential step method coupled with UV-Vis spectroscopy, was used to evaluate their EC properties: switching times, optical contrasts, changes of the optical densities and colouration efficiencies. In Figure 6 are depicted the chronoabsorptograms obtained for poly[1] films ($\Gamma$ = 0.16 μmol $cm^{-2}$) in $LiClO_4/CH_3CN$ and $LiClO_4$/PC, for the two colour changes - yellow ↔ green (λ=750 nm) and green ↔ russet (λ=510 nm). The results obtained for poly[2] ($\Gamma$ = 0.84 μmol $cm^{-2}$) in a similar study are depicted in Figure S6, SI and, in Figure S7, are depicted the UV-Vis spectra for the two films in each colour and in both supporting electrolytes, with identification of the considered wavelengths.

Figure 6

The switching times ($\tau$), estimated from absorbance-time curves and indicated in Figures 6 and S6, were determined considering 90% of the full optical change.[19,21] The switching time values obtained in $LiClO_4/CH_3CN$ are $\tau$ = 9 / 10 s for the yellow ↔ green transition for both poly[1] and poly[2] and $\tau$ = 10 / 13 and 8 / 9 s for the green ↔ russet transition of poly[1] and poly[2], respectively. In $LiClO_4$/PC, the switching time values are $\tau$ = 13 / 14 s for poly[1] and $\tau$ = 14 / 15 s for poly[2], in the case of the yellow ↔ green transition, whereas $\tau$ = 14 / 24 and 9 / 11 s for the green ↔ russet transition of poly[1] and poly[2], respectively, being clearly higher than those determined in $LiClO_4/CH_3CN$. The higher switching times observed in $LiClO_4$/PC can be related with the lower degree of PC film solvation that may hamper the $ClO_4^-$ counter-ions ingress, necessary to the charge balance during redox switching. This assumption is in agreement with the XPS results (Table 1), which revealed a larger increase in O/Ni ratio, from the reduced to the oxidized state, in $LiClO_4/CH_3CN$ than in $LiClO_4$/PC. Furthermore, independently of the electrolyte solution employed, the colour transition yellow ↔ green is the fastest for poly[1], while for poly[2] is the green ↔ russet transition. The switching time values suggested that these films are especially useful for applications in which the demand for rapid switching is smaller, as in slow-acting electronic devices,[12] such as smart cards or labels.

As a complementary result, in Figure S8 are depicted, as an example, the chronoamperograms/chronocoulograms obtained simultaneously with the chronoabsorptograms for the colour transition yellow ↔ green for poly[1] film in $LiClO_4$/PC. It is possible to see that the switching time values estimated from current intensity and charge are similar to the values determined from absorbance. In fact, from the results, it is seen that the absorbance variation with the redox switching is reflected in the chronoamperograms by a current decay as the potential become constant (indicating

that at each time a portion of the film is undergoing a redox process);[19] the charge represents the same information in integrated form. The strong couple between these parameters highlight the possibility of the use of the current intensity / charge profiles as accurate parameters to evaluate the switching times of these polymeric films.

In Table 3 are summarised the optical contrasts, changes of the optical density, charges requirements and colouration efficiencies values, determined for the two films colour changes in both electrolyte solutions. The optical contrast, defined as the transmittance difference, $\Delta T$ %, between redox states,[23] was measured from the chronoabsorptograms, considering the full optical change. For poly[1] film in $LiClO_4/CH_3CN$, the optical contrast for the colour transition yellow ↔ green is higher than for the green ↔ russet transition ($\Delta T$ = 44.9 % vs. 32.7 %). In $LiClO_4$/PC, the optical contrasts decrease for both colour changes ($\Delta T$ = 26.2% and 18.3 %, respectively). The poly[2] film have an opposite behaviour: the colour transition green ↔ russet has a higher contrast than the yellow ↔ green transition ($\Delta T$ = 19.4 % vs. 13.0 %), being that in $LiClO_4$/PC the contrasts are enhanced (for $\Delta T$ = 58.5 % and 51.2 %). The measured optical contrasts are in accordance with colours difference observed on photographs of Figure 5.

The change of the optical density, ΔOD, was estimated using the Equation 2. For both polymeric films, the ΔOD values for the yellow ↔ green colour transition are very similar in $LiClO_4/CH_3CN$ and $LiClO_4$/PC. For the green ↔ russet transitions, on the other hand, the ΔOD are significantly lower in $LiClO_4$/PC (for poly[1], ΔOD = 0.92 in $LiClO_4/CH_3CN$ and 0.53 in $LiClO_4$/PC). These results reflect the behaviour of the obtained UV-Vis spectra represented on Figures 4, S2 or S7. The smaller ΔOD value in $LiClO_4$/PC is in accordance with the decrease of the intensity of the band at λ=510 – 525 from $LiClO_4/CH_3CN$ to the $LiClO_4$/PC electrolyte solution (as discussed in section 3.3),

providing an indication that the green ↔ russet colour change is mainly associated with the appearance of the band at λ=510 - 525 nm, attributed to CT transitions. For the remaining UV-Vis bands, no significant differences were observed in the two electrolyte solutions, which is consistent with the similar ΔOD values for the yellow ↔ green colour change.

The power efficiency of the EC films was measured through the colouration efficiency, $\eta$, determined by Equation 3, considering the $Q_d$ values obtained from the chronocoulograms, as represented in Figure S8 (b) for poly[1] in $LiClO_4$/PC. The $\eta$ values measured are in range 33.14 – 83.18 $cm^2\ C^{-1}$ for the colour transition yellow ↔ green and 84.12 – 152.04 for the green ↔ russet transition. The higher values for the green ↔ russet transition can be explained by the induced higher ΔOD, with similar or even lower charge requirements. Furthermore, for a same colour change, the films presented smaller $\eta$ values in $LiClO_4$/PC electrolyte. Comparing both films, poly[1] showed better colouration efficiency. However, it is important to note that Equation 3 is typically used for the characterization of bleached to coloured switching materials. Consequently, EC materials that exhibit transitions within the visible region, as in these films, tend to lower the $\eta$ values, although can reflect into modest optical changes.[12]

The electrochemical stability of poly[Ni(*salen*)] films were evaluated by chronoamperometric observations, investigating the influence of the electrolyte solutions - $LiClO_4/CH_3CN$ or $LiClO_4$/PC – on the cycle life of yellow ↔ green and green ↔ russet colour transitions. The obtained chronoamperograms are depicted in Figure 7 for poly[1] and in Figure S9 for poly[2]; in the figures are also indicated the percentage of charge loss, corresponding to the number of redox cycles after which no further colour change was observable.

Figure 7

Independently of the colour change, both polymeric films showed greater electrochemical stability in $LiClO_4$/PC than in $LiClO_4$/$CH_3CN$. The best stability was obtained for poly[1] film in $LiClO_4$/PC that changed colour between yellow and green during around 9000 redox cycles with a charge loss of 34.3 %. The same film, in $LiClO_4$/$CH_3CN$, showed colour change only during around 2000 redox cycles, with a charge intensity loss of 60.0 %. The green ↔ russet colour transition was less stable: after 400 redox cycles poly[1] showed a loss in charge intensity of 96.1 % in $LiClO_4$/$CH_3CN$ and 68.2 % in $LiClO_4$/PC.

Moreover, for the yellow ↔ green change poly[2] showed charge intensities losses of 10.5 % and 70.9 % in $LiClO_4$/PC and $LiClO_4$/$CH_3CN$, respectively, at around 650 redox cycles (taking in account that, for this film, the colour contrast between the yellow and green is low). The green ↔ russet change, although showed the highest contrast for this film, also revealed to be unstable, with charge intensity losses of 70.2 % in $LiClO_4$/PC and 88.6 % in $LiClO_4$/$CH_3CN$ (at 650 cycles). These results showed that poly[2] has an inferior electrochemical stability performance than poly[1]. Furthermore, the reasons for the general better stabilities in $LiClO_4$/PC are not well known, but can be related with the less volatility of PC compared to $CH_3CN$ and with degradation of the substrate (PET) over time, when immersed in $CH_3CN$.

In Table S4 are summarized the switching times determined for both poly[Ni(*salen*)] films during the stability studies, along the redox cycles. Note that these response times are in general higher than those indicated on Figures 6, S6 and S8, because the films used here were deposited during 10 scans ($\Gamma \approx 0.31$ and 1.13 μmol $cm^{-2}$, for poly[1] and poly[2], respectively), while the films used in chronoabsorptometric studies

were deposited during 5 scans ($\Gamma \approx 0.16$ and 0.84 μmol cm$^{-2}$, for poly[1] and poly[2], respectively) and, so, have different thicknesses. In a general way, the response times for the colour changes yellow – green and green – russet (oxidation processes) tend to increase slightly or remain nearly constant, while the response times for the colour changes green – yellow and russet – green (reduction processes) tend to decrease slightly or remain constant.

The electrochemical stability of poly[1] film in $LiClO_4$/PC was also evaluated by CV during 200 redox cycles (Figure S10). The voltammetric responses showed that the anodic peak corresponding to the process associated with the colour change from the yellow to green ($E_{pa}$ = 0.37 V) shifted to more positive potentials along the successive redox cycles, suggesting morphological and/or structural changes in film matrix. On the other hand, the anodic peak corresponding to the process associated with the colour change from green to russet ($E_{pa}$ = 0.99 V) showed a more rapid decrease in current intensity, reaching very low values. At this point, the anodic peak at more positive potential values was overlapped by the peak associated with the yellow to green colour change, such that this became the dominant observed colour change. These observations can justify the lower stability of the green ↔ russet colour change.

Taking into account the diversity of ligands already used in the design of poly[Ni(*salen*)] films, it can be concluded that the high electrochemical stability obtained for poly[1] results from the presence of σ-donor methyl groups in the 3-position of the salicylaldehyde moieties; furthermore, the presence of four methyl groups in the imine bridge had a negative effect on the electrochemical stability of previously studied poly[Ni(*salen*)] films.

It can be recognised that the electrochemical stability of poly[Ni(*salen*)] films resulted from a subtle combination of substituents effects in the imine bridge and/or in

the 3-position of the salicylaldehyde moiety: substituents in the 5-position of salicylaldehyde moieties prevent polymerization and positions 4- and 6- have lower effect on the overall stability since they are not directly conjugated with the C-O-Ni moiety. Although no chronoamperometric studies have been made for previously studied poly[Ni(*salen*)] films, the voltammetric studies suggested that poly[Ni(salen)] (pristine salen, no substituents) showed lower stability than poly[Ni(saltMe)] [47] (pristine salen with four methyl groups in the imine bridge − σ-donors) and poly[Ni(3-MeOsaltMe)] [48] (pristine saltMe with methoxy group − π donor and σ-withdraw group − in the 3-position of the salicylaldehyde moiety). In this context, the choice of *salen* ligands with a σ-donor methyl group in the 3-position of the salicylaldehyde moieties, individually, and combined with four methyl groups in the imine bridge could account for high stability in the oxidised state, provided by the electron σ-donor properties of the methyl groups. However, the four methyl groups in the imine bridge may also have a significant impact on the supramolecular polymer structure (difficult to anticipate) due to the different conformations for the ethylene backbone in the imine bridge, that can favour/disfavour the film electrochemical stability; in the present study it disfavoured poly[2] electrochemical stability.

As a summary, the high electrochemical stability obtained for poly[1] in $LiClO_4$/PC electrolyte solution constitutes a step forward in the electrochemical stability improvement when compared with others poly[M(*salen*)] films,[35-36] and highlights the potentiality of this film as a very stable EC material. Furthermore, when compared with other EC materials, poly[1] in $LiClO_4$/PC showed faster responses (lower switching times) than the inorganic metal oxides (typically, $\tau$ = 12-60 s),[37,42] and similar or even higher optical contrasts and colouration efficiencies than some conducting polymers and derived composites.[20,38,49]

### 3.5 ECDs fabrication and characterization

The high electrochemical stability of the colour change yellow ↔ green of the poly[1], allied with its good optical contrast, makes it the choice for the fabrication of a solid-state ECD; in the case of poly[2], although the high optical contrast associated with the green ↔ russet colour change could be a key issue in the selection for ECD fabrication, its low electrochemical stability remains the highest important drawback. Thereby, ECDs was fabricated using poly[1] as EC material using a lateral configuration, in two figures of merit: a simple shape (typology 1) and a butterfly shape (typology 2); the latter to exploit the possibility of a future application in smart cards or labels.

In Figure 8 are presented the pictures and schematic illustrations of the assembled ECDs. In both typologies, the electrodes are in the same plane and are designated by 1 or 2: the electrode 1 is in the reduced state and showed a yellow colour, while electrode 2 is in the oxidized state and exhibited a green colour.

Figure 8

In Figure 9 (a) are depicted the chronoamperograms obtained during the study of the electrochemical stability of the ECD of typology 1, considering the colour change yellow ↔ green. The ECD retained a clear change colour for ca. 3000 redox cycles, with a loss in charge intensity of 37.0 %.

Figure 9

During the first 1000 redox cycles, the process was simultaneously monitored by *in situ* UV-Vis spectroscopy, at λ=750 nm (Figure 9 (b)). At the end of these cycles, the ECD registered a charge loss of 23.1 % and a loss of 15.8 % in absorbance. The estimated $\tau$ values are reported in Figure 9 (c). From the absorbance – time curves, $\tau$ = 157 s for the colour change yellow – green and $\tau$ = 145s for the reverse colour change. These times are similar to those determined from the chronoamperograms: $\tau$ = 151 and 142 s to the yellow – green and green – yellow colour changes, respectively. Furthermore, the optical contrast of the assembled ECD was calculated as $\Delta T$ = 88.7 % (at λ = 750 nm) and the colouration efficiency as $\eta$ = 130.4 $cm^2$ $C^{-1}$, with ΔOD = 0.84 and a charge requirement of the $Q_d$ = 6.4 mC $cm^{-2}$.

In order to evaluate the application of this EC system in devices with more sophisticated template forms, a proof-of-concept ECD of typology 2 was assembled. The electrochemical stability of the ECD of typology 2 was determined through the chronoamperograms depicted in Figure S11. The ECD changed of colour between yellow and green during around 1250 redox cycles, with a charge loss of 58.9 %. These results indicate the need for a more optimized typology when more sophisticated ECD templates are needed in terms of future applications.

## 4. CONCLUSIONS

Poly[1] and poly[2] films were successfully electrodeposited on ITO/PET flexible substrates. Voltammetric characterization revealed that poly[1] showed similar redox profiles in $LiClO_4/CH_3CN$ and $LiClO_4$/PC, while poly[2] showed solvent dependent electrochemical responses. Both films showed multielectrochromic behaviour, exhibiting yellow, green and russet colours, according to their oxidation state.

EC properties were firstly studied in solution with both polymer films showing switching times in the range 8 - 24 seconds; this is consistent with their potential application in slow-acting electronic devices. For poly[1], the yellow ↔ green colour transition showed the best optical contrast, whereas for poly[2] it was the green ↔ russet transition. Poly[1] also showed the best colouration efficiencies, with the highest values being obtained for the green ↔ russet colour change. Both polymeric films were more electrochemically stable in $LiClO_4$/PC, although the overall poorer electrochemically stability of poly[2]: the highest electrochemical stability was obtained for the yellow ↔ green change in poly[1] in $LiClO_4$/PC, with charge intensity loss of only 34.3 % after 9000 cycles. Consequently, poly[1] was used to fabricate ECD with two figures of merit (typology 1 and 2), with typology 1 showing the best performance: $\Delta T$ = 88.7 % (at $\lambda$ = 750 nm), $\eta$ = 130.4 $cm^2\ C^{-1}$, charge intensity decrease of 37.0 % after 3000 redox cycles.

The results showed that poly[1] has promising EC properties both in a solution cell and in a solid-state device. Combination of high electrochemical stability, interesting poly-electrochromism and good optical contrast motivate the application of poly[1] as EC material in electronic displays. Furthermore, the combination of these EC properties with a flexible substrate has considerable advantages that may be exploited in paper-like applications.

**Supporting Information**

Summary of the peak potentials observed in CVs, XPS data for poly[2] and XPS spectra in O1s region, UV-Vis data for poly[1], differential UV-Vis spectra and *Abs* vs. *Q* plots, chronoabsorptograms / amperograms / coulograms for poly[1] and poly[2], estimated switching times and chronoamperograms of the ECD of typology 2.

**ACKNOWLEDGMENTS**

The authors thank Fundação para a Ciência e a Tecnologia (FCT, Portugal) and FEDER under Programme PT2020 (UID/QUI/50006/2013). MN (SFRH/BD/79171/2011) and MA (SFRH/BD/89156/2012) also thank FCT for their grants.

## *REFERENCES*


1. Deb, S. K., A Novel Electrophotographic System. *Applied Optics* **1969,** *8 Suppl 1*, 192-195.
2. Lian, W. R.; Huang, Y. C.; Liao, Y. A.; Wang, K. L.; Li, L. J.; Su, C. Y.; Liaw, D. J.; Lee, K. R.; Lai, J. Y., Flexible Electrochromic Devices Based on Optoelectronically Active Polynorbornene Layer and Ultratransparent Graphene Electrodes. *Macromolecules* **2011,** *44* (24), 9550-9555.
3. Caglar, A.; Cengiz, U.; Yildirim, M.; Kaya, I., Effect of Deposition Charges on the Wettability Performance of Electrochromic Polymers. *Appl. Surf. Sci.* **2015,** *331*, 262-270.
4. Reyes-Gil, K. R.; Stephens, Z. D.; Stavila, V.; Robinson, D. B., Composite $WO_3/TiO_2$ Nanostructures for High Electrochromic Activity. *ACS Appl. Mater. Interfaces* **2015,** *7* (4), 2202-2213.
5. Granqvist, C. G., Electrochromics for Smart Windows: Oxide-Based Thin Films and Devices. *Thin Solid Films* **2014,** *564*, 1-38.
6. Mortimer, R. J.; Varley, T. S., In Situ Spectroelectrochemistry and Colour Measurement of a Complementary Electrochromic Device Based on Surface-Confined Prussian Blue and Aqueous Solution-Phase Methyl Viologen. *Sol. Energy Mater. Sol. Cells* **2012,** *99*, 213-220.
7. Abaci, U.; Guney, H. Y.; Kadiroglu, U., Morphological and Electrochemical Properties of PPy, PAni Bilayer Films and Enhanced Stability of Their Electrochromic Devices (PPy/PANI-PEDOT, PANI/PPy-PEDOT). *Electrochim. Acta* **2013,** *96*, 214-224.
8. Saikia, D.; Pan, Y. C.; Wu, C. G.; Fang, J.; Tsai, L. D.; Kao, H. M., Synthesis and Characterization of a Highly Conductive Organic-Inorganic Hybrid Polymer Electrolyte Based on Amine Terminated Triblock Polyethers and its Application in Electrochromic Devices. *J. Mater. Chem. C* **2014,** *2* (2), 331-343.
9. Sydam, R.; Deepa, M.; Shivaprasad, S. M.; Srivastava, A. K., A $WO_3$-Poly(Butyl Viologen) Layer-by-Layer Film/Ruthenium Purple Film Based Electrochromic Device Switching by 1 Volt Application. *Sol. Energy Mater. Sol. Cells* **2015,** *132*, 148-161.
10. Osterholm, A. M.; Shen, D. E.; Kerszulis, J. A.; Bulloch, R. H.; Kuepfer, M.; Dyer, A. L.; Reynolds, J. R., Four Shades of Brown: Tuning of Electrochromic Polymer Blends Toward High-Contrast Eyewear. *ACS Appl. Mater. Interfaces* **2015,** *7* (3), 1413-1421.
11. Li, K. R.; Zhang, Q. H.; Wang, H. Z.; Li, Y. G., Red, Green, Blue (RGB) Electrochromic Fibers for the New Smart Color Change Fabrics. *ACS Appl. Mater. Interfaces* **2014,** *6* (15), 13043-13050.
12. Beaujuge, P. M.; Reynolds, J. R., Color Control in π-Conjugated Organic Polymers for Use in Electrochromic Devices. *Chem. Rev.* **2010,** *110* (1), 268-320.
13. Argun, A. A.; Reynolds, J. R., Line Patterning for Flexible and Laterally Configured Electrochromic Devices. *J. Mater. Chem.* **2005,** *15* (18), 1793-1800.
14. Thakur, V. K.; Ding, G. Q.; Ma, J.; Lee, P. S.; Lu, X. H., Hybrid Materials and Polymer Electrolytes for Electrochromic Device Applications. *Adv. Mater.* **2012,** *24* (30), 4071-4096.
15. Schott, M.; Lorrmann, H.; Szczerba, W.; Beck, M.; Kurth, D. G., State-of-the-Art Electrochromic Materials Based on Metallo-Supramolecular Polymers. *Sol. Energy Mater. Sol. Cells* **2014,** *126*, 68-73.
16. Kraft, A.; Rottmann, M., Properties, Performance and Current Status of the Laminated Electrochromic Glass of Gesimat. *Sol. Energy Mater. Sol. Cells* **2009,** *93* (12), 2088-2092.
17. Gillaspie, D. T.; Tenent, R. C.; Dillon, A. C., Metal-Oxide Films for Electrochromic Applications: Present Technology and Future Directions. *J. Mater. Chem.* **2010,** *20* (43), 9585-9592.
18. Sydam, R.; Deepa, M.; Joshi, A. G., A Novel 1,1 '-Bis 4-(5,6-Dimethyl-1H-Benzimidazole-1-yl)Butyl-4,4'-Bipyridinium Dibromide (Viologen) for a High Contrast Electrochromic Device. *Org. Electron.* **2013,** *14* (4), 1027-1036.
19. Amb, C. M.; Dyer, A. L.; Reynolds, J. R., Navigating the Color Palette of Solution-Processable Electrochromic Polymers. *Chemistry of Materials* **2011,** *23* (3), 397-415.

20. Yu, W. Y.; Chen, J.; Fu, Y. L.; Xu, J. K.; Nie, G. M., Electrochromic Property of a Copolymer Based on 5-Cyanoindole and 3,4-Ethylenedioxythiophene and its Application in Electrochromic Devices. *J. Electroanal. Chem.* **2013,** *700*, 17-23.
21. Wu, T. Y.; Liao, J. W.; Chen, C. Y., Electrochemical Synthesis, Characterization and Electrochromic Properties of Indan and 1,3-Benzodioxole-Based Poly(2,5-Dithienylpyrrole) Derivatives. *Electrochim. Acta* **2014,** *150*, 245-262.
22. Rende, E.; Kilic, C. E.; Udum, Y. A.; Toffoli, D.; Toppare, L., Electrochromic Properties of Multicolored Novel Polymer Synthesized Via Combination of Benzotriazole and N-Functionalized 2,5-di(2-Thienyl)-1H-Pyrrole Units. *Electrochim. Acta* **2014,** *138*, 454-463.
23. Chang, K. H.; Wang, H. P.; Wu, T. Y.; Sun, I. W., Optical and Electrochromic Characterizations of Four 2,5-Dithienylpyrrole-Based Conducting Polymer Films. *Electrochim. Acta* **2014,** *119*, 225-235.
24. Jarosz, T.; Brzeczek, A.; Walczak, K.; Lapkowski, M.; Domagala, W., Multielectrochromism of Redox States of Thin Electropolymerised Films of Poly(3-Dodecylpyrrole) Involving a Black Coloured State. *Electrochim. Acta* **2014,** *137*, 595-601.
25. Kurtay, G.; Ak, M.; Gullu, M.; Toppare, L.; Ak, M. S., Synthesis and Electropolymerization of 3,4-Substituted Quinoxaline Functionalized Pyrrole Monomer and Optoelectronic Properties of its Polymer. *Synth. Met.* **2014,** *194*, 19-28.
26. Lu, J. L.; Liu, W. S.; Ling, H.; Kong, J. H.; Ding, G. Q.; Zhou, D.; Lu, X. H., Layer-by-layer Assembled Sulfonated-Graphene/Polyaniline Nanocomposite Films: Enhanced Electrical and Ionic Conductivities and Electrochromic Properties. *RSC Adv.* **2012,** *2* (28), 10537-10543.
27. Sydam, R.; Kokal, R. K.; Deepa, M., Fast, Direct, Low-Cost Route to Scalable, Conductive, and Multipurpose Poly(3,4-Ethylenedixoythiophene)-Coated Plastic Electrodes. *ChemPhysChem* **2015,** *16* (5), 1042-1051.
28. Xiong, S. X.; Fu, J. L.; Li, Z. F.; Shi, Y. J.; Wang, X. Q.; Chu, J.; Gong, M.; Wu, B. H., Modulating the Electrochromic Performances of Transmissive and Reflective Devices Using N, N-Dimethyl Formamide Modified Poly(3,4-Ethylenedioxythiophene)/Poly(Styrene Sulfonate) Blend as Active Layers. *J. Macromol. Sci., Part B: Phys.* **2015,** *54* (7), 799-810.
29. Kang, J. H.; Oh, Y. J.; Paek, S. M.; Hwang, S. J.; Choy, J. H., Electrochromic Device of PEDOT-PANI Hybrid System for Fast Response and High Optical Contrast. *Sol. Energy Mater. Sol. Cells* **2009,** *93* (12), 2040-2044.
30. Sydorov, D.; Duboriz, I.; Pud, A., Poly(3-Methylthiophene)-Polyaniline Couple Spectroelectrochemistry Revisited for the Complementary Red-Green-Blue Electrochromic Device. *Electrochim. Acta* **2013,** *106*, 114-120.
31. Kraft, A.; Rottmann, M.; Gilsing, H. D.; Faltz, H., Electrodeposition and Electrochromic Properties of N-Ethyl Substituted Poly (3,4-Ethylenedioxypyrrole). *Electrochim. Acta* **2007,** *52* (19), 5856-5862.
32. Fonseca, J.; Tedim, J.; Biernacki, K.; Magalhaes, A. L.; Gurman, S. J.; Freire, C.; Hillman, A. R., Structural and Electrochemical Characterisation of Pd(salen)-Type Conducting Polymer Films. *Electrochim. Acta* **2010,** *55* (26), 7726-7736.
33. Vilas-Boas, M.; Santos, I. C.; Henderson, M. J.; Freire, C.; Hillman, A. R.; Vieil, E., Electrochemical Behavior of a New Precursor for the Design of Poly Ni(salen)-Based Modified Electrodes. *Langmuir* **2003,** *19* (18), 7460-7468.
34. Martins, M.; Boas, M. V.; de Castro, B.; Hillman, A. R.; Freire, C., Spectroelectrochemical Characterisation of Copper Salen-Based Polymer-Modified Electrodes. *Electrochim. Acta* **2005,** *51* (2), 304-314.
35. Pinheiro, C.; Parola, A. J.; Pina, F.; Fonseca, J.; Freire, C., Electrocolorimetry of Electrochromic Materials on Flexible ITO Electrodes. *Sol. Energy Mater. Sol. Cells* **2008,** *92* (8), 980-985.
36. Branco, A.; Pinheiro, C.; Fonseca, J.; Tedim, J.; Carneiro, A.; Parola, A. J.; Freire, C.; Pina, F., Solid-State Electrochromic Cells Based on M(salen)-Derived Electroactive Polymer Films. *Electrochem. Solid State Lett.* **2010,** *13* (9), J114-J118.

37. Kalagi, S. S.; Mali, S. S.; Dalavi, D. S.; Inamdar, A. I.; Im, H.; Patil, P. S., Limitations of Dual and Complementary Inorganic-Organic Electrochromic Device for Smart Window Application and its Colorimetric Analysis. *Synth. Met.* **2011,** *161* (11-12), 1105-1112.
38. Xu, G. Q.; Zhao, J. S.; Cui, C. S.; Hou, Y. F.; Kong, Y., Novel Multicolored Electrochromic Polymers Containing Phenanthrene-9,10-Quinone and Thiophene Derivatives Moieties. *Electrochim. Acta* **2013,** *112*, 95-103.
39. Freire, C.; de Castro, B., Spectroscopic Characterisation of Electrogenerated Nickel(III) Species. Complexes with $N_2O_2$ Schiff-Base Ligands Derived from Salicylaldehyde. *J. Chem. Soc., Dalton Trans.* **1998,** (9), 1491-1497.
40. Tedim, J.; Patricio, S.; Fonseca, J.; Magalhaes, A. L.; Moura, C.; Hillman, A. R.; Freire, C., Modulating Spectroelectrochemical Properties of Ni(salen) Polymeric Films at Molecular Level. *Synth. Met.* **2011,** *161* (9-10), 680-691.
41. Dale, S. M.; Glidle, A.; Hillman, A. R., Spectroelectrochemical Observation of Poly(Benzo-Thiophene) N-Doping and P-Doping. *J. Mater. Chem.* **1992,** *2* (1), 99-104.
42. Sapp, S. A.; Sotzing, G. A.; Reynolds, J. R., High Contrast Ratio and Fast-Switching Dual Polymer Electrochromic Devices. *Chem. Mat.* **1998,** *10* (8), 2101-2108.
43. Tedim, J.; Carneiro, A.; Bessada, R.; Patricio, S.; Magalhaes, A. L.; Freire, C.; Gurman, S. J.; Hillman, A. R., Correlating Structure and Ion Recognition Properties of Ni(salen)-Based Polymer Films. *J. Electroanal. Chem.* **2007,** *610* (1), 46-56.
44. Tedim, J.; Goncalves, F.; Pereira, M. F. R.; Figueiredo, J. L.; Moura, C.; Freire, C.; Hillman, A. R., Preparation and Characterization of Poly Ni(salen)(Crown Receptor)/Multi-Walled Carbon Nanotube Composite Films. *Electrochim. Acta* **2008,** *53* (23), 6722-6731.
45. Dahm, C. E.; Peters, D. G.; Simonet, J., Electrochemical and Spectroscopic Characterization of Anodically Formed Nickel Salen Polymer Films on Glassy Carbon, Platinum, and Optically Transparent Tin Oxide Electrodes in Acetonitrile Containing Tetramethylammonium Tetrafluoroborate. *J. Electroanal. Chem.* **1996,** *410* (2), 163-171.
46. Vilas-Boas, M.; Freire, C.; de Castro, B.; Christensen, P. A.; Hillman, A. R., Spectroelectrochemical Characterisation of Poly Ni(saltMe)-Modified Electrodes. *Chem.-Eur. J.* **2001,** *7* (1), 139-150.
47. Vilas-Boas, M.; Freire, C.; de Castro, B.; Hillman, A. R., Electrochemical Characterization of a Novel Salen-Type Modified Electrode. *J. Phys. Chem. B* **1998**, *102* (43), 8533-8540.
48. Vilas-Boas, M.; Santos, I. C.; Henderson, M. J.; Freire, C.; Hillman, A. R.; Vieil, E.,Electrochemical Behavior of a New Precursor for the Design of Poly[Ni(salen)]-Based Modified Electrodes. *Langmuir* **2003**, *19* (18), 7460-7468.
49. Camurlu, P.; Gultekin, C.; Bicil, Z., Fast switching, High Contrast Multichromic Polymers from Alkyl-Derivatized Dithienylpyrrole and 3,4-Ethylenedioxythiophene. *Electrochim. Acta* **2012,** *61*, 50-56.

**Table 1:** XPS results for poly[1]: surface atomic percentages and atomic ratios for reduced and oxidised polymeric films in $LiClO_4/CH_3CN$ and $LiClO_4$/PC 0.1 mol $dm^{-3}$.

| Films | Atomic % | | | | | Atomic Ratios | | |
|---|---|---|---|---|---|---|---|---|
| | Ni | C | N | O | Cl | N/Ni | O/Ni | Cl/Ni |
| **$LiClO_4/CH_3CN$** | | | | | | | | |
| Reduced state | 3.31 | 78.60 | 7.89 | 10.03 | 0.16 | 2.38 | 3.03 | 0.05 |
| Oxidised state | 1.76 | 60.52 | 6.06 | 26.33 | 5.32 | 3.44 | 14.96 | 3.02 |
| **$LiClO_4$/PC** | | | | | | | | |
| Reduced state | 2.87 | 76.41 | 6.93 | 12.66 | 0.87 | 2.41 | 4.41 | 0.30 |
| Oxidised state | 2.51 | 71.31 | 6.55 | 17.39 | 2.23 | 2.61 | 6.93 | 0.89 |

**Table 2:** Electronic bands and respective molar extinction coefficients ($\varepsilon$) for poly[1] and poly[2] in $LiClO_4/CH_3CN$ and $LiClO_4/PC$.

| Film | Electrolyte solution | $\lambda_{max}$ / nm (eV) | $\varepsilon \times 10^{-3}$ / $mol^{-1}\ dm^3\ cm^{-1}$ |
|---|---|---|---|
| **poly[1]** | $LiClO_4/CH_3CN$ | 327 (3.79) | 4.99 |
| | | 402 (3.09) | 3.06 |
| | | 510 (2.43) | 19.66 |
| | | 843 (1.47) | 5.21 |
| | $LiClO_4/PC$ | 327 (3.79) | 5.90 |
| | | 402 (3.09) | 3.12 |
| | | 510 (2.43) | 13.64 |
| | | 843 (1.47) | 6.72 |
| **poly[2]** | $LiClO_4/CH_3CN$ | 330 (3.76) | 0.76 |
| | | 415 (2.99) | 0.42 |
| | | 525 (2.36) | 4.22 |
| | | > 950 (1.31) | 0.68 |
| | $LiClO_4/PC$ | 330 (3.76) | 0.60 |
| | | 415 (2.99) | 0.31 |
| | | 520 (2.39) | 1.37 |
| | | 639 (1.94) | 0.64 |
| | | > 950 (1.31) | 0.54 |

**Table 3:** EC parameters for poly[1] and poly[2] films in $LiClO_4/CH_3CN$ and $LiClO_4$/PC: optical contrasts ($\Delta T$ %), changes of the optical density ($\Delta$OD), charge requirements ($Q_d$), and colouration efficiencies ($\eta$).

| Film | Electrolyte solution | Colour transition [a)] | $\Delta T$ % | $\Delta$OD | $Q_d$ / mC cm$^{-2}$ | $\eta$ / cm$^2$ C$^{-1}$ |
|---|---|---|---|---|---|---|
| **poly[1]** | $LiClO_4/CH_3CN$ | yellow ↔ green | 44.9 | 0.47 | 5.62 | 83.18 |
| | | green ↔ russet | 32.7 | 0.92 | 6.05 | 152.04 |
| | $LiClO_4$/PC | yellow ↔ green | 26.2 | 0.49 | 6.46 | 75.55 |
| | | green ↔ russet | 18.3 | 0.53 | 4.92 | 107.36 |
| **poly[2]** | $LiClO_4/CH_3CN$ | yellow ↔ green | 13.0 | 0.11 | 2.99 | 36.94 |
| | | green ↔ russet | 19.4 | 0.36 | 2.42 | 146.86 |
| | $LiClO_4$/PC | yellow ↔ green | 51.2 | 0.13 | 4.02 | 33.14 |
| | | green ↔ russet | 58.5 | 0.32 | 3.80 | 84.12 |

[a)] $\lambda$=510 nm and $\lambda$=750 nm for the colour transitions green ↔ russet and yellow ↔ green, respectively.

# CAPTIONS TO FIGURES

**Figure 1.** CVs of the electrodeposition of (a) [Ni(3-Mesalen)] and (b) [Ni(3-MesaltMe)] complexes in ITO/PET, using 1.0 mmol $dm^{-3}$ solutions of complexes in $LiClO_4/CH_3CN$ 0.1 mol $dm^{-3}$, at 0.02 V $s^{-1}$ during 10 cycles. Inset: chemical structures of the respective [Ni(*salen*)] complex.

**Figure 2.** Voltammetric responses of (a) poly[1] ($\Gamma$ = 0.31 μmol $cm^{-2}$) and (b) poly[2] ($\Gamma$ = 1.13 μmol $cm^{-2}$) films in $LiClO_4/CH_3CN$ (panel A) and $LiClO_4$/PC (panel B) 0.1 mol $dm^{-3}$ electrolytes, acquiring at the scan rate of 0.02 V $s^{-1}$.

**Figure 3.** SEM micrographs and respective EDS spectra at selected zones for poly[1] films in (a) reduced and (b) oxidised states, with a magnification of 20000 times.

**Figure 4.** Panel A: Absolute UV-Visible spectra of poly[1] ($\Gamma$ = 0.16 μmol $cm^{-2}$) acquired during film oxidation in 0.1 mol $dm^{-3}$ (a) $LiClO_4/CH_3CN$ and (b) $LiClO_4$/PC (referenced to respective electrolytes spectra; ─ spectra at -0.1 V, ─ spectra at 1.3 V). Panel B: *Abs* vs. *E* plots for electronic bands identified in absolute UV-Vis spectra, referenced to spectra at -0.1 V (arrows indicate scan direction).

**Figure 5.** Photographs of (a) poly[1] and (b) poly[2] films in different oxidation states (0.0 V, 0.7 V and 1.3 V vs. Ag/AgCl (NaCl / 1.0 mol.$dm^{-3}$)) in $LiClO_4/CH_3CN$ electrolyte.

**Figure 6.** Chronoabsorptograms for poly[1] films in $LiClO_4/CH_3CN$ (—) and $LiClO_4$/PC (—), for the colour transitions (a) yellow ↔ green (λ=750 nm) and (b) green ↔ russet (λ=510 nm), with indication of the estimated switching times.

**Figure 7.** Chronoamperograms of poly[1] films in $LiClO_4/CH_3CN$ (—) and $LiClO_4$/PC (—) for the colour changes (a) yellow ↔ green and (b) green ↔ russet, applying two potential pulses of 50 s by redox cycle, with potential alternating between (a) 0.0 - 0.7 V and (b) 0.7 – 1.3 V.

**Figure 8.** Pictures (Panel A) and schematic illustrations (Panel B) of the assembled ECDs of (a and a') typology 1 and (b and b') typology 2, showing the colour contrast between the two electrodes, each one in different oxidation states: electrode 1 in reduced state (-1.0 V and -1.1 V) and electrode 2 in oxidized state (1.0 V and -0.25 V); in (b') the cut to prevent the electrical contact corresponds to the butterfly's shape / borders and the connection to the potential source is made through the link between the butterfly's wing and the clean surface of ITO.

**Figure 9.** ECD of typology 1: (a) chronoamperograms obtained by the application of two potential pulses of 200 s by redox cycle, with potential alternating between -1.0 (yellow) and 1.0 V (green); chronoabsorptograms (at $\lambda = 750$ nm) and respective chronoamperograms obtained during (b) the first 1000 redox cycles and (c) the first three redox cycles, with indication of the switching times.

**Figure 1.**

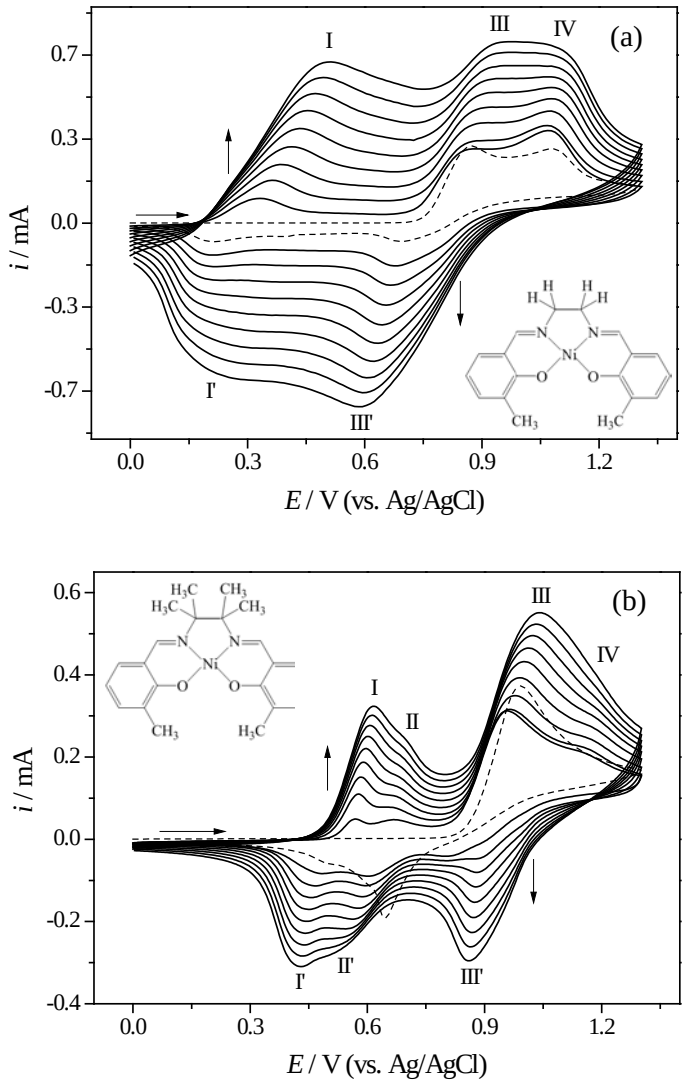
(a)
I
III
IV
I'
III'
i / mA
E / V (vs. Ag/AgCl)
(b)
I
II
III
IV
I'
II'
III'
i / mA
E / V (vs. Ag/AgCl)

**Figure 2.**

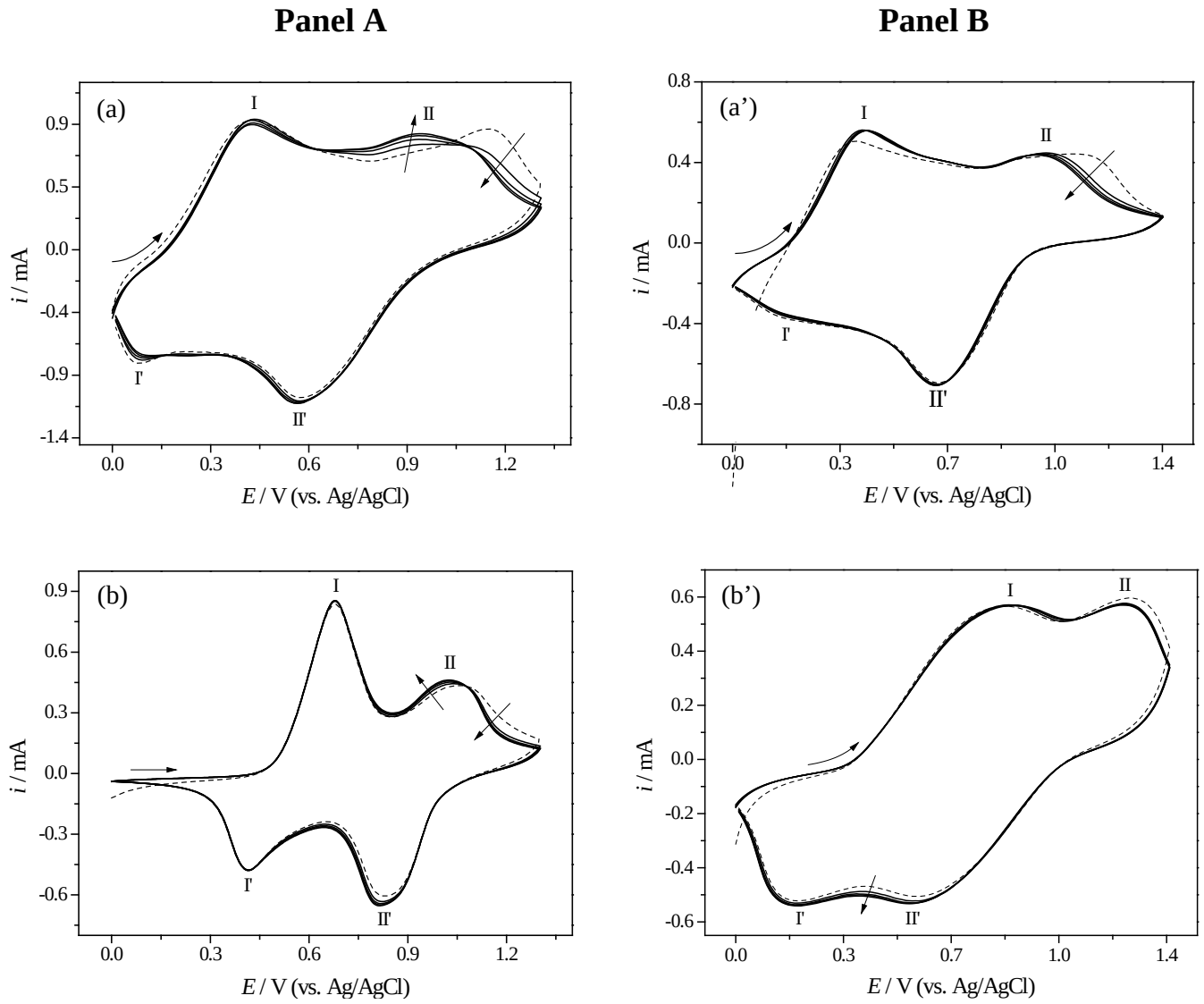

**Figure 3.**

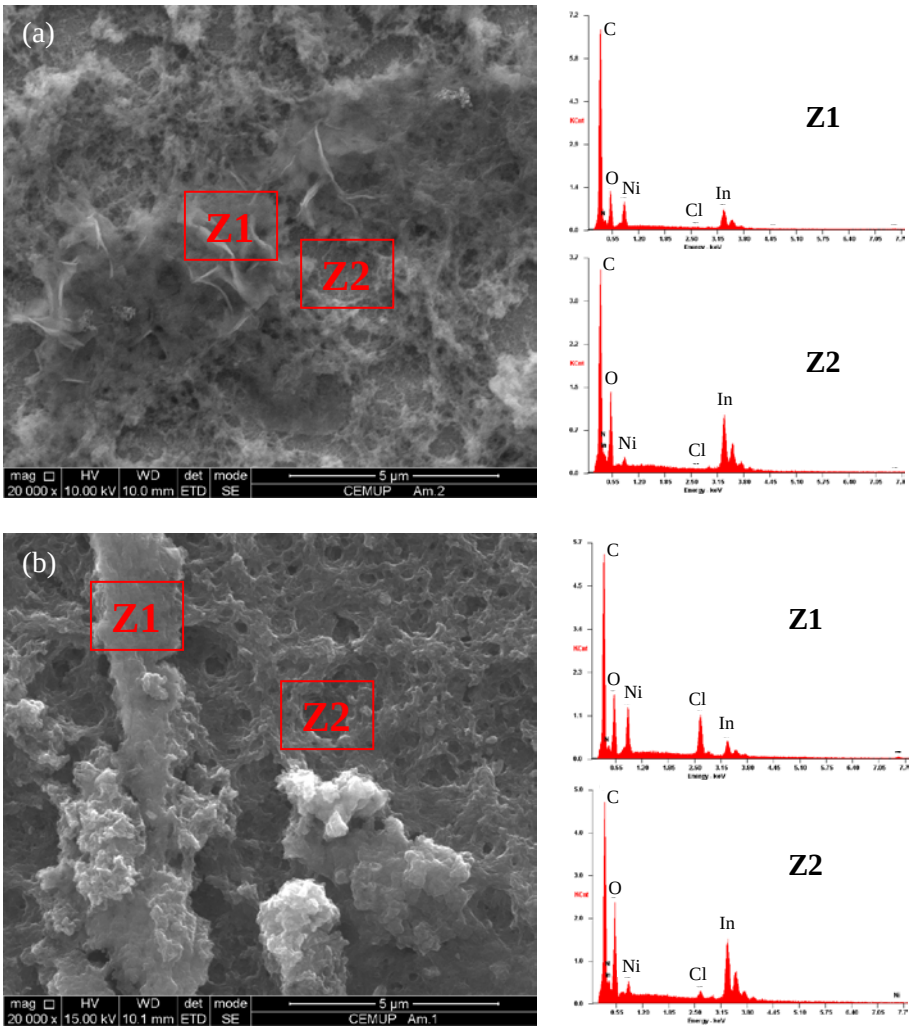
(a)
Z1
Z2
mag HV WD det mode
20 000 x 10.00 kV 10.0 mm ETD SE
5 µm
CEMUP Am.2
C
O
Ni
Cl
In
Z1
C
O
Ni
Cl
In
Z2
(b)
Z1
Z2
mag HV WD det mode
20 000 x 15.00 kV 10.1 mm ETD SE
5 µm
CEMUP Am.1
C
O
Ni
Cl
In
Z1
C
O
Ni
Cl
In
Z2

**Figure 4.**

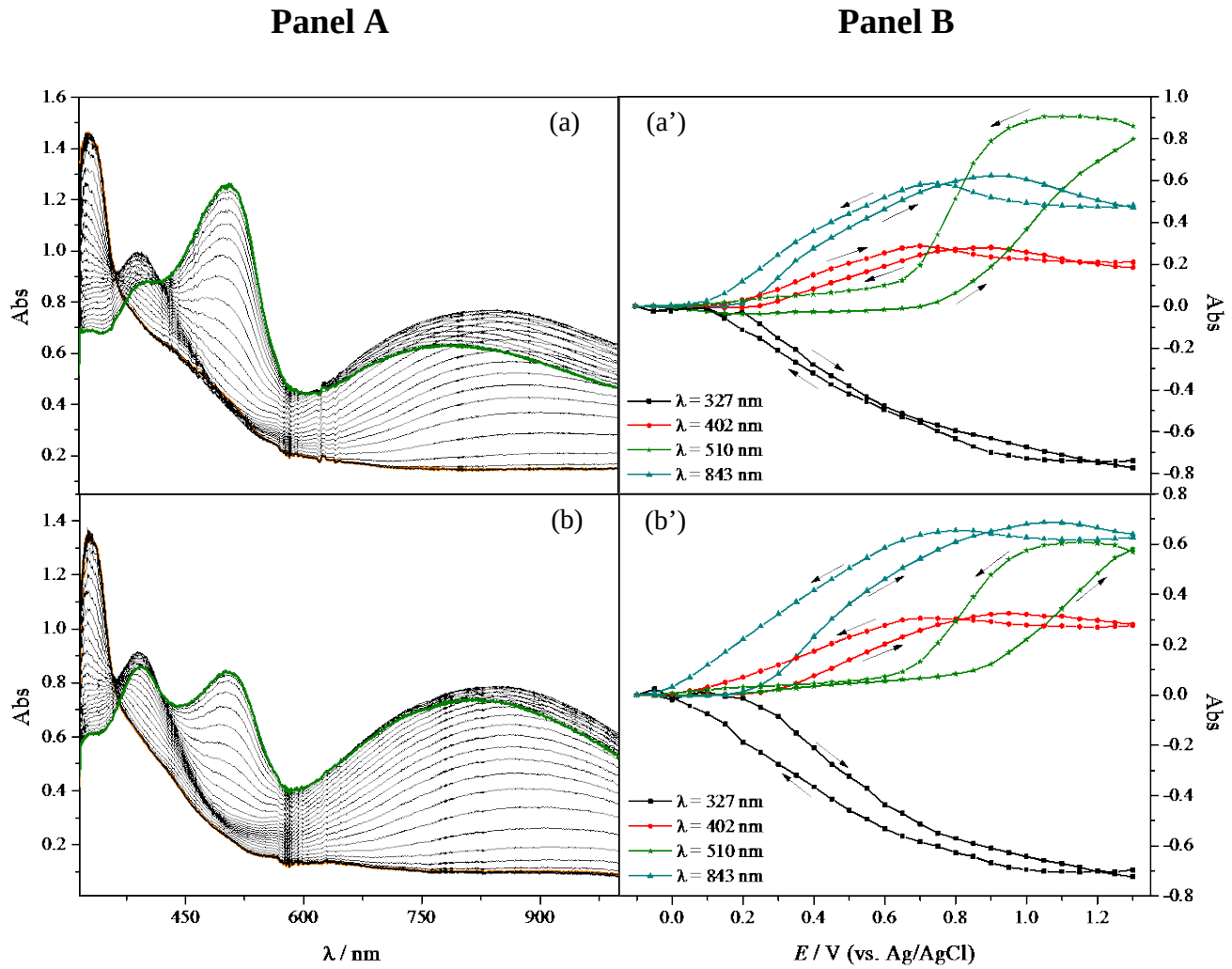
Panel A
Panel B
(a)
(a')
(b)
(b')
Abs
λ / nm
E / V (vs. Ag/AgCl)
λ = 327 nm
λ = 402 nm
λ = 510 nm
λ = 843 nm

**Figure 5.**

(a)

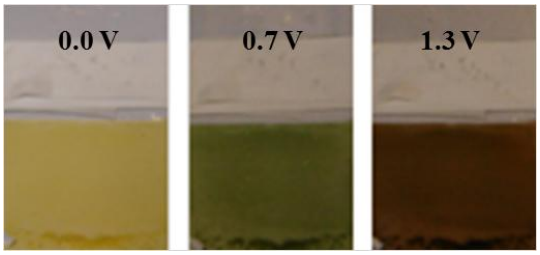


(b)

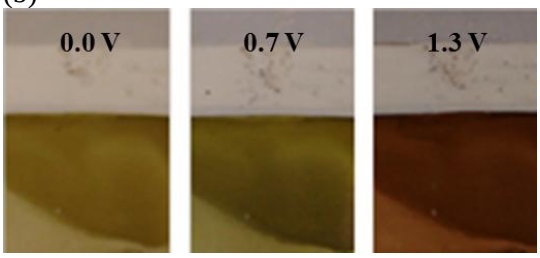

**Figure 6.**

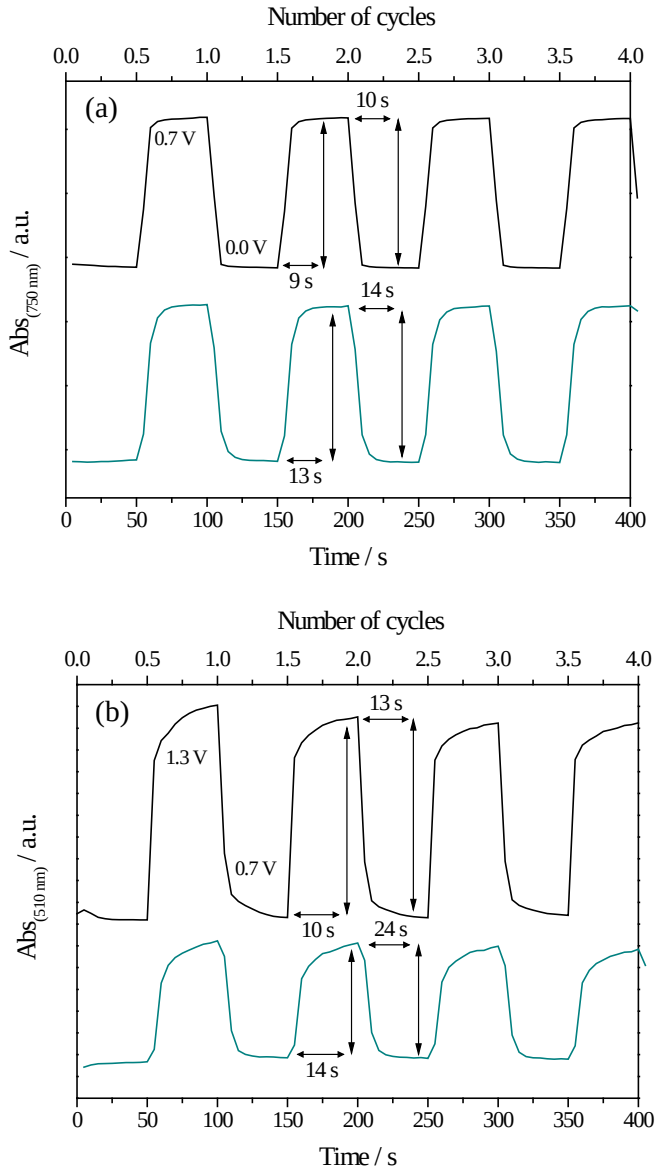
Number of cycles
0.0 0.5 1.0 1.5 2.0 2.5 3.0 3.5 4.0
(a)
0.7 V
0.0 V
10 s
9 s
14 s
13 s
Abs(750 nm) / a.u.
0 50 100 150 200 250 300 350 400
Time / s
Number of cycles
0.0 0.5 1.0 1.5 2.0 2.5 3.0 3.5 4.0
(b)
1.3 V
0.7 V
13 s
10 s
24 s
14 s
Abs(510 nm) / a.u.
0 50 100 150 200 250 300 350 400
Time / s

**Figure 7.**

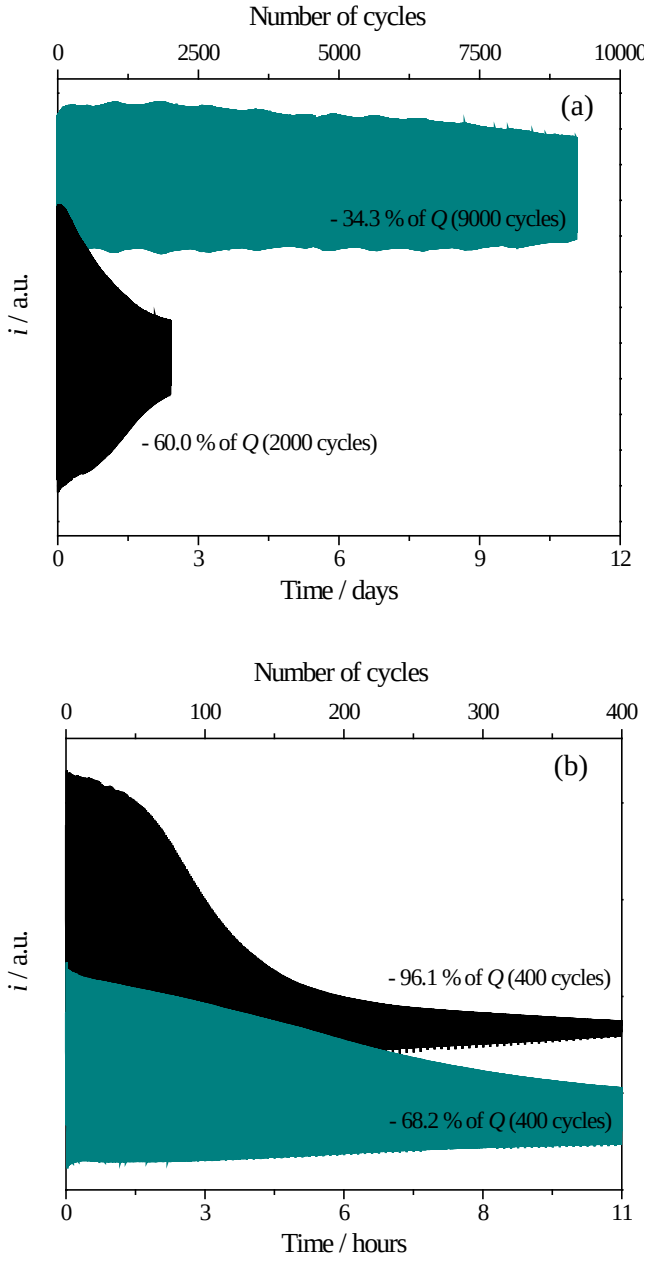
Number of cycles
0
2500
5000
7500
10000
(a)
- 34.3 % of Q (9000 cycles)
- 60.0 % of Q (2000 cycles)
i / a.u.
0
3
6
9
12
Time / days
Number of cycles
0
100
200
300
400
(b)
- 96.1 % of Q (400 cycles)
- 68.2 % of Q (400 cycles)
i / a.u.
0
3
6
8
11
Time / hours

**Figure 8.**

**Panel A** **Panel B**

(a)

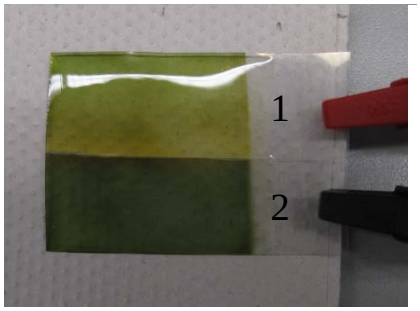


(a')

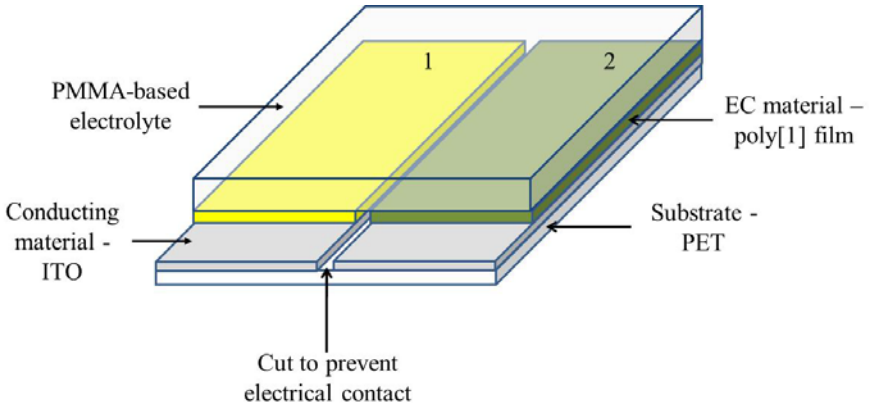


(b)

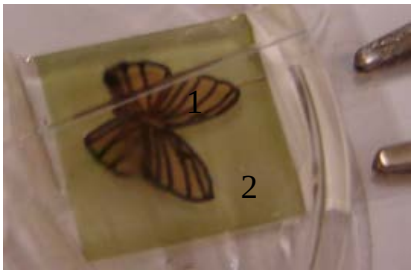


(b')

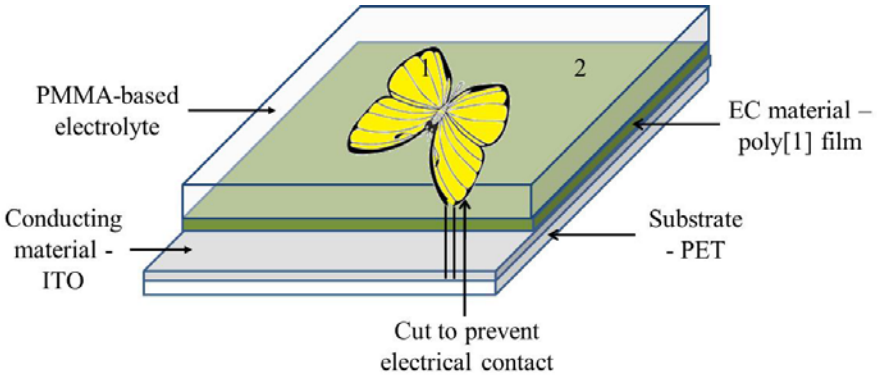

**Figure 9.**

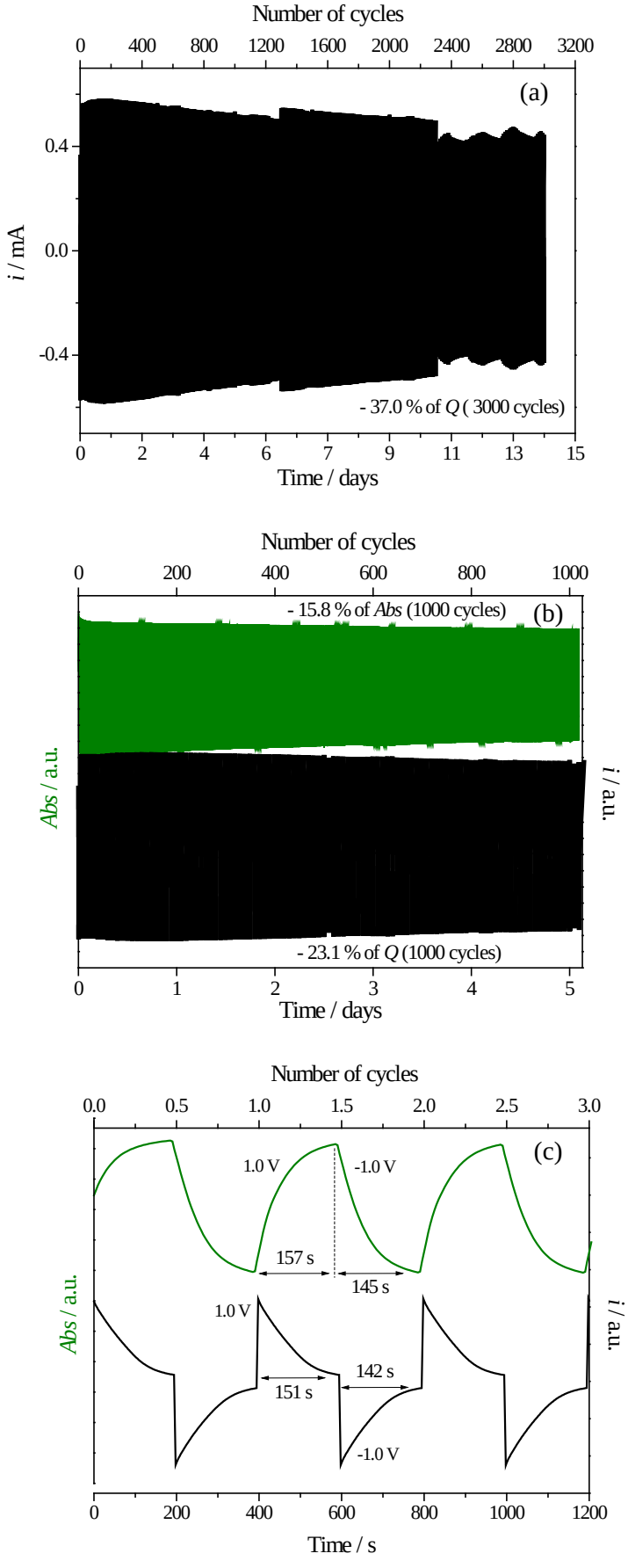
Number of cycles
0 400 800 1200 1600 2000 2400 2800 3200
(a)
0.4
0.0
-0.4
i / mA
- 37.0 % of Q ( 3000 cycles)
0 2 4 6 7 9 11 13 15
Time / days
Number of cycles
0 200 400 600 800 1000
- 15.8 % of Abs (1000 cycles)
(b)
Abs / a.u.
i / a.u.
- 23.1 % of Q (1000 cycles)
0 1 2 3 4 5
Time / days
Number of cycles
0.0 0.5 1.0 1.5 2.0 2.5 3.0
(c)
1.0 V
-1.0 V
157 s
145 s
1.0 V
142 s
151 s
-1.0 V
Abs / a.u.
i / a.u.
0 200 400 600 800 1000 1200
Time / s

**SUPPORTING INFORMATION**

# High-performance electrochromic devices based on poly[Ni(*salen*)]-type polymer films

Marta Nunes,[a] Mariana Araújo,[a] Joana Fonseca,[b] Cosme Moura,[c] Robert Hillman[d] and Cristina Freire[a*]

[a] REQUIMTE/LAQV, Departamento de Química e Bioquímica, Faculdade de Ciências, Universidade do Porto, 4169-007 Porto, Portugal

[b] CeNTI, Rua Fernando Mesquita, 2785, 4760-034 Vila Nova de Famalicão, Portugal

[c] CIQ, Departamento de Química e Bioquímica, Faculdade de Ciências, Universidade do Porto, 4169-007 Porto, Portugal

[d] Department of Chemistry, University of Leicester, Leicester LE1 7 RH, UK

*Corresponding author: Dr. Cristina Freire; e-mail: acfreire@fc.up.pt
Tel.: +351 22 04020590; Fax: +351 22 0402 695.

**Table S1:** Peak potentials in CVs during 1st and 5th scans of films electrodeposition.

| Films | *E* / V (vs Ag/AgCl) | | | | | | | |
|---|---|---|---|---|---|---|---|---|
| | **Scan** | $E_{paI}$ | $E_{paII}$ | $E_{paIII}$ | $E_{paIV}$ | $E_{pcI'}$ | $E_{pcII'}$ | $E_{pcIII'}$ |
| **poly[1]** | 1st | - | - | 0.87 | 1.08 | 0.20 | - | 0.69 |
| | 5th | 0.42 | - | 0.91 | 1.08 | 0.22 | - | 0.64 |
| **poly[2]** | 1st | - | - | 0.99 | - | 0.50 | 0.64- | - |
| | 5th | 0.59 | 0.68 | 0.99 | 1.17 | 0.45 | 0.58 | 0.87 |

**Table S2:** Peak potentials in CVs during 1st and 5th scans of films redox switching.

| Films | Supporting Electrolyte solution | *E* / V (vs Ag/AgCl) | | | | |
|---|---|---|---|---|---|---|
| | | Scan | $E_{paI}$ | $E_{paII}$ | $E_{pcI'}$ | $E_{pcII'}$ |
| poly[1] | $LiClO_4/CH_3CN$ | 1st | 0.42 | 1.16 | 0.18 | 0.58 |
| | | 5th | 0.42 | 0.94 | 0.17 | 0.56 |
| | $LiClO_4$/PC | 1st | 0.39 | 1.16 | 0.20 | 0.66 |
| | | 5th | 0.43 | 1.00 | 0.20 | 0.66 |
| poly[2] | $LiClO_4/CH_3CN$ | 1st | 0.68 | 1.07 | 0.41 | 0.83 |
| | | 5th | 0.68 | 1.03 | 0.41 | 0.81 |
| | $LiClO_4$/PC | 1st | 0.87 | 1.29 | 0.19 | 0.58 |
| | | 5th | 0.88 | 1.27 | 0.19 | 0.56 |

**Table S3:** XPS surface atomic percentages and atomic ratios for reduced and oxidised poly[2] films in $LiClO_4$/PC 0.1 mol $dm^{-3}$.

| Films | Atomic % | | | | | Atomic Ratios | | |
|---|---|---|---|---|---|---|---|---|
| | **Ni** | **C** | **N** | **O** | **Cl** | **N/Ni** | **O/Ni** | **Cl/Ni** |
| Reduced state | 2.55 | 76.69 | 6.13 | 12.26 | 0.81 | 2.40 | 4.81 | 0.32 |
| Oxidised state | 1.89 | 65.98 | 5.78 | 22.76 | 3.28 | 3.06 | 12.04 | 1.74 |

**Table S4:** Switching times measured along the chronoamperometric studies for poly[1] and poly[2] in $LiClO_4/CH_3CN$ and $LiClO_4/PC$ (Figures 7 and S9).

| Films | Supporting Electrolyte solution | Switching times / s | | | | | |
|---|---|---|---|---|---|---|---|
| | | Number of cycles | yellow - green | green - yellow | Number of cycles | green - russet | russet - green |
| poly[1] | $LiClO_4/CH_3CN$ | 0 | 9.3 | 8.4 | 0 | 6.9 | 25.0 |
| | | 1000 | 11.3 | 6.4 | 100 | 11.7 | 24.2 |
| | | 2000 | 24.0 | 7.6 | 200 | 29.8 | 17.8 |
| | $LiClO_4/PC$ | 0 | 20.6 | 15.4 | 0 | 10.5 | 36.02 |
| | | 1000 | 16.5 | 16.6 | 100 | 9.9 | 30.37 |
| | | 2000 | 16.6 | 17.2 | 200 | 11.8 | 29.9 |
| | | 3000 | 17.5 | 16.7 | 300 | 14.9 | 30.2 |
| | | 6000 | 17.4 | 13.2 | | | |
| | | 9000 | 17.9 | 9.9 | | | |
| poly[2] | $LiClO_4/CH_3CN$ | 0 | 9.9 | 3.3 | 0 | 20.78 | 14.3 |
| | | 200 | 10.8 | 3.7 | 100 | - | 11.3 |
| | $LiClO_4/PC$ | 0 | 38.8 | 12.1 | 0 | 23.9 | 30.5 |
| | | 200 | 39.1 | 12.2 | 100 | 17.2 | 24.9 |
| | | 400 | 39.5 | 12.0 | 200 | 19.9 | 24.7 |
| | | 600 | 38.8 | 12.0 | 300 | 20.0 | 22.0 |

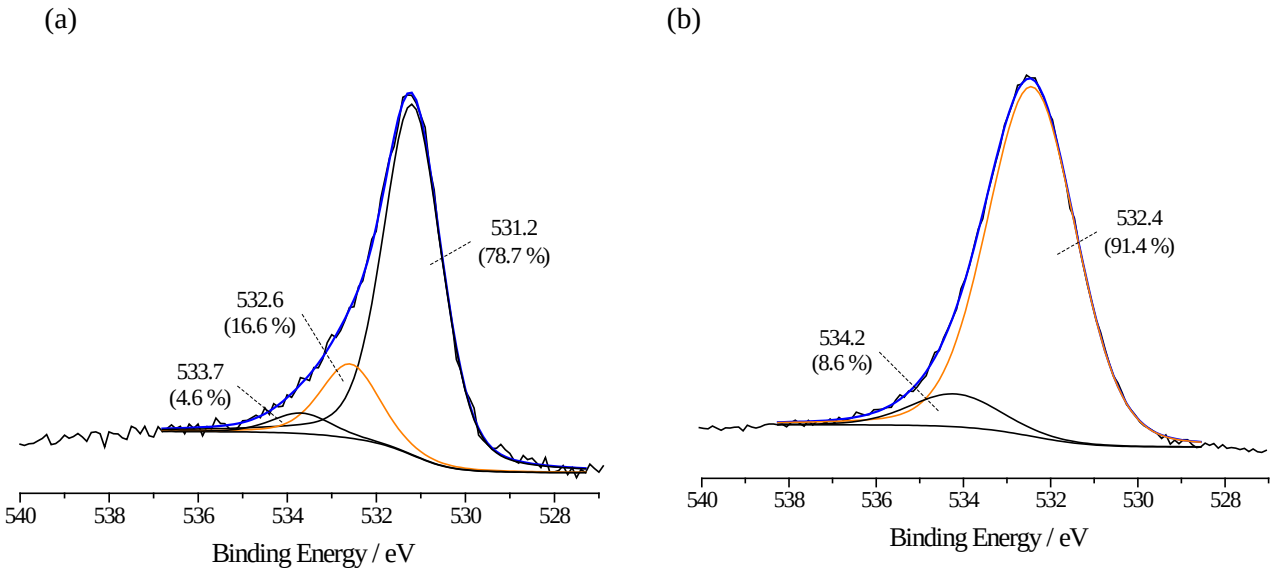


**Figure S1.** High-resolution XPS spectra in O 1s region of poly[1] film in (a) reduced and (b) oxidised states in $LiClO_4/CH_3CN$, with respective deconvolutions; — peak assigned to $ClO_4^-$.

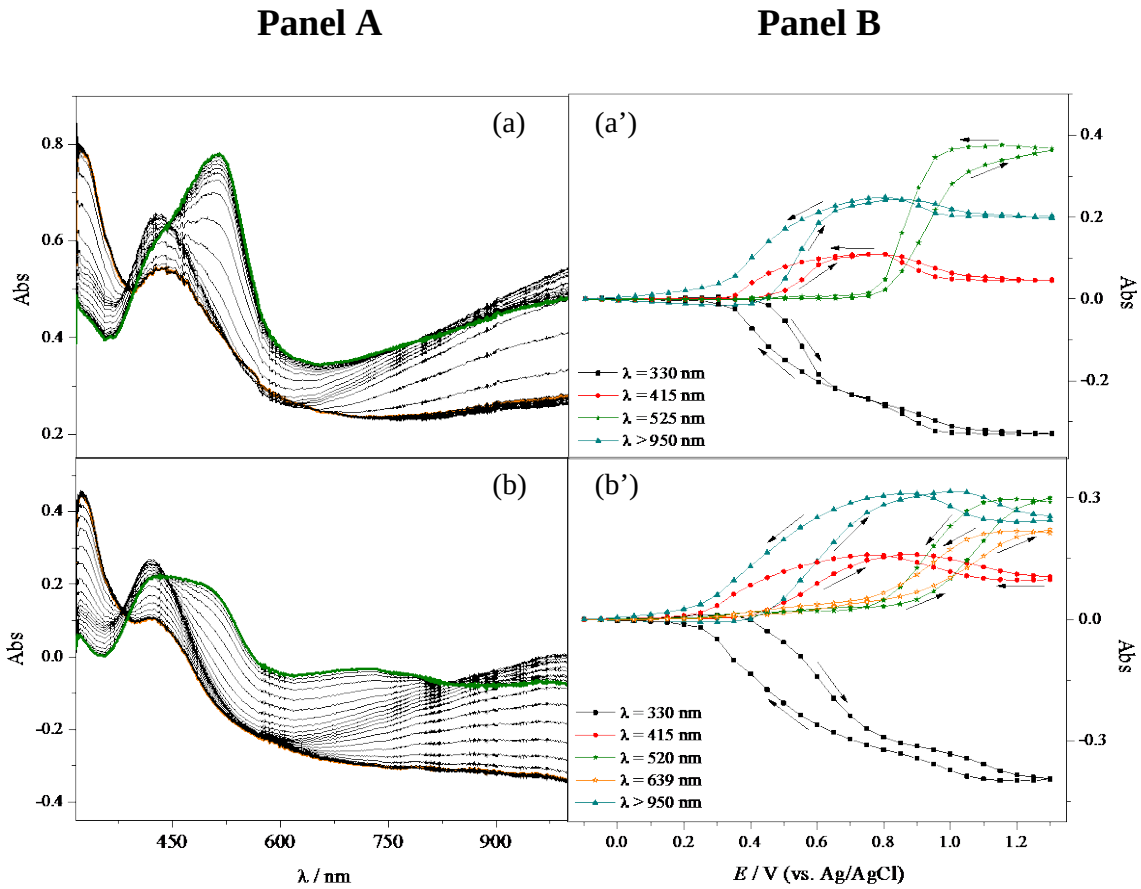


**Figure S2.** Panel A: Absolute UV-Visible spectra of poly[2] ($\Gamma$ = 0.84 μmol cm$^{-2}$) acquired during film oxidation in 0.1 mol dm$^{-3}$ (a) $LiClO_4/CH_3CN$ and (b) $LiClO_4$/PC (referenced to respective electrolytes; — spectra at -0.1 V, — spectra at 1.3 V). Panel B: *Abs* vs. *E* plots for electronic bands identified in absolute UV-Vis spectra, referenced to spectra at -0.1 V (arrows indicate scan direction).

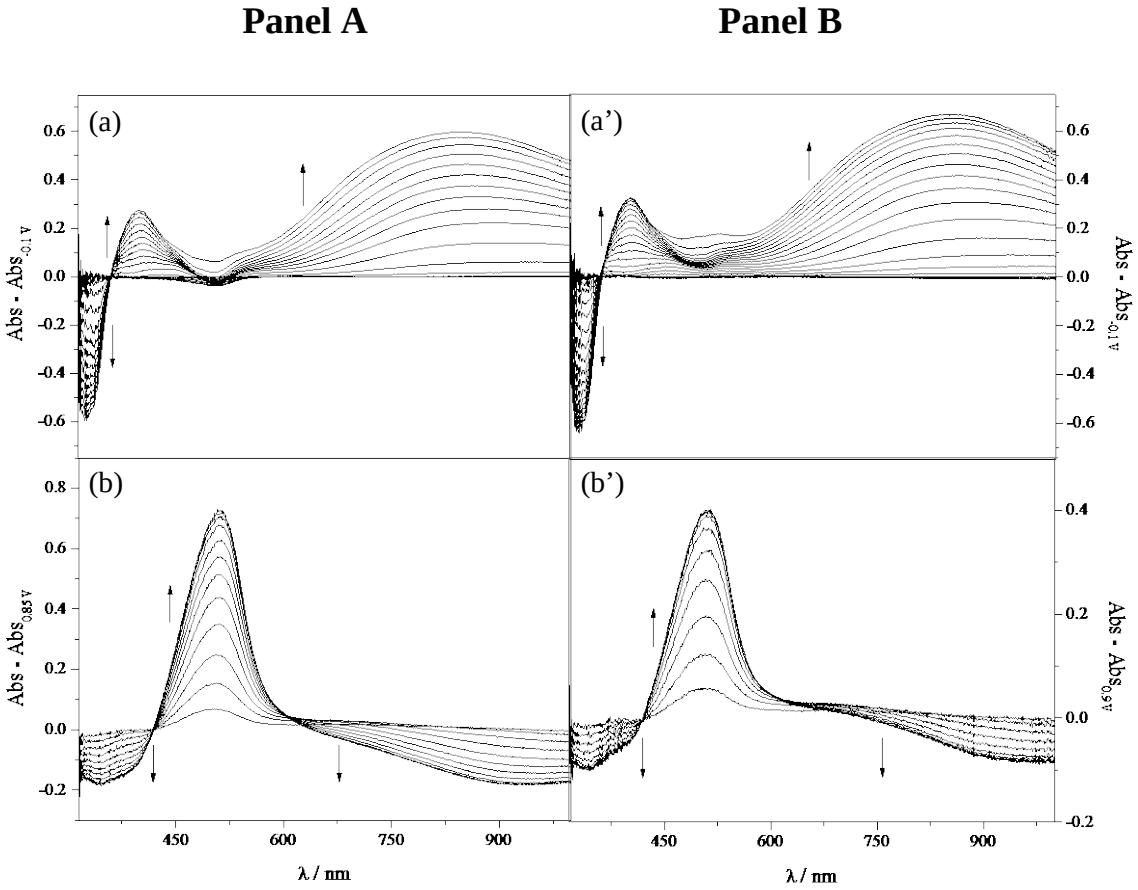


**Figure S3.** UV-Visible spectra of poly[1] ($\Gamma$ = 0.16 μmol cm$^{-2}$) acquired during the film oxidation in $LiClO_4/CH_3CN$ (Panel A) and $LiClO_4$/PC (Panel B) from (a) -0.1 to 0.85 V and referenced to the spectrum of neutral polymer, (b) 0.85 to 1.3 V and referenced to the spectrum of the polymer at 0.85 V, (a') -0.1 to 0.9 V and referenced to the spectrum of neutral polymer and (b') 0.9 to 1.3 V and referenced to the spectrum of the polymer at 0.9 V.

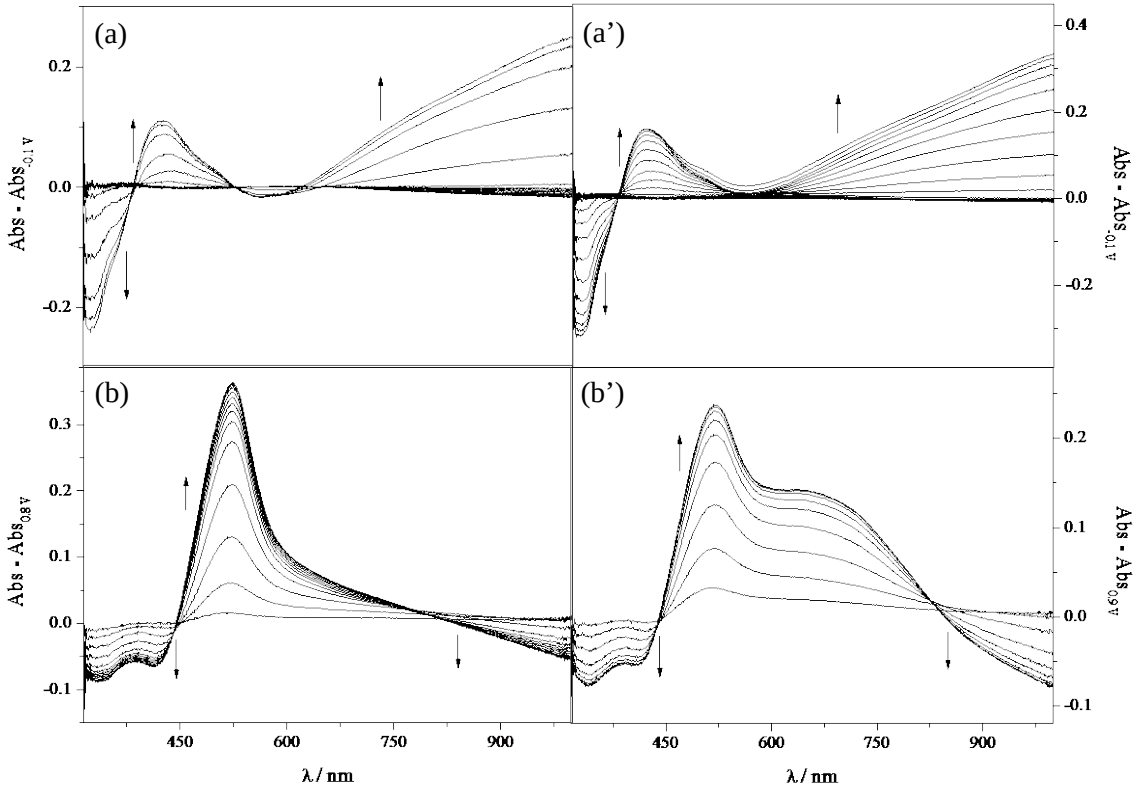


**Figure S4.** UV-Visible spectra of poly[2] ($\Gamma$ = 0.84 μmol cm$^{-2}$) acquired during the film oxidation in $LiClO_4/CH_3CN$ (Panel A) and $LiClO_4$/PC (Panel B) from (a) -0.1 to 0.8 V and referenced to the spectrum of neutral polymer, (b) 0.8 to 1.3 V and referenced to the spectrum of the polymer at 0.8 V, (a') -0.1 to 0.9 V and referenced to the spectrum of neutral polymer and (b') 0.9 to 1.3 V and referenced to the spectrum of the polymer at 0.9 V.

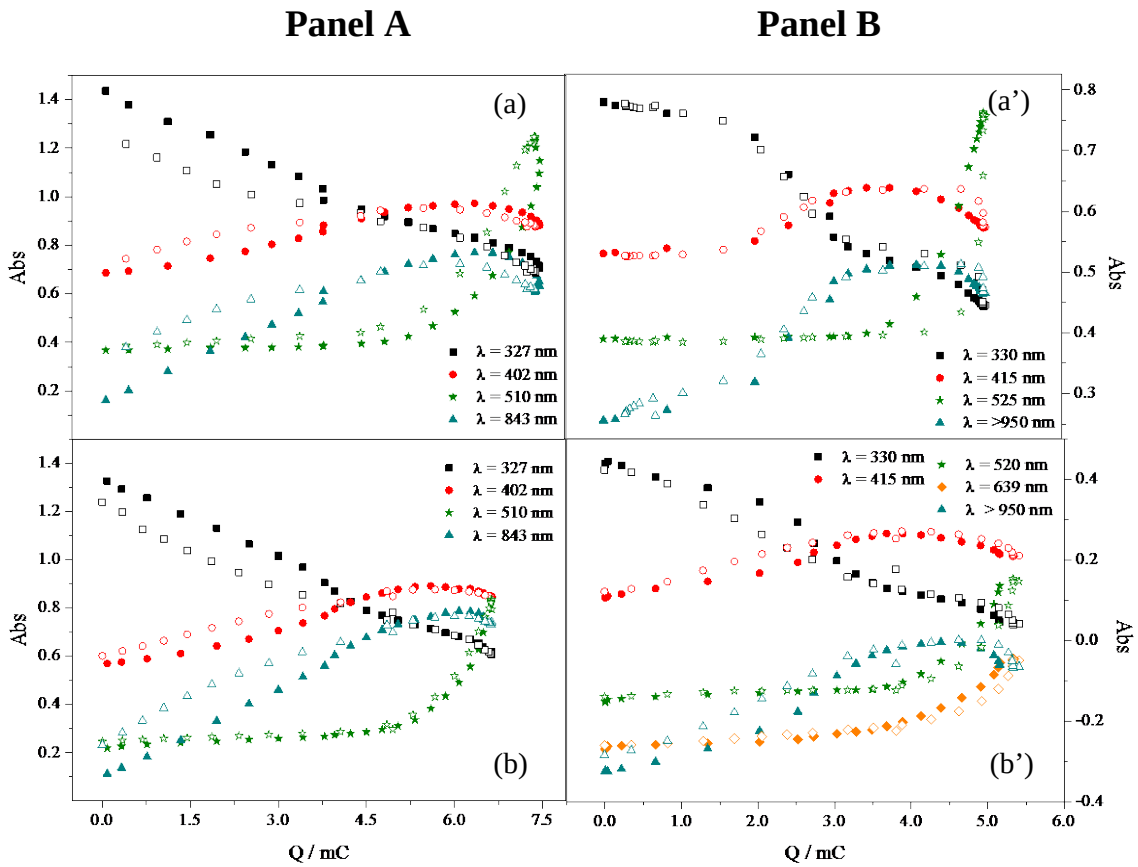


**Figure S5.** Plots of the *Abs* vs. *Q* for selected electronic bands for poly[1] (Panel A) and poly[2] (Panel B) in $LiClO_4/CH_3CN$ (a and a') and $LiClO_4$/PC (b and b'); filled forms correspond to anodic scan and open forms to cathodic scan.

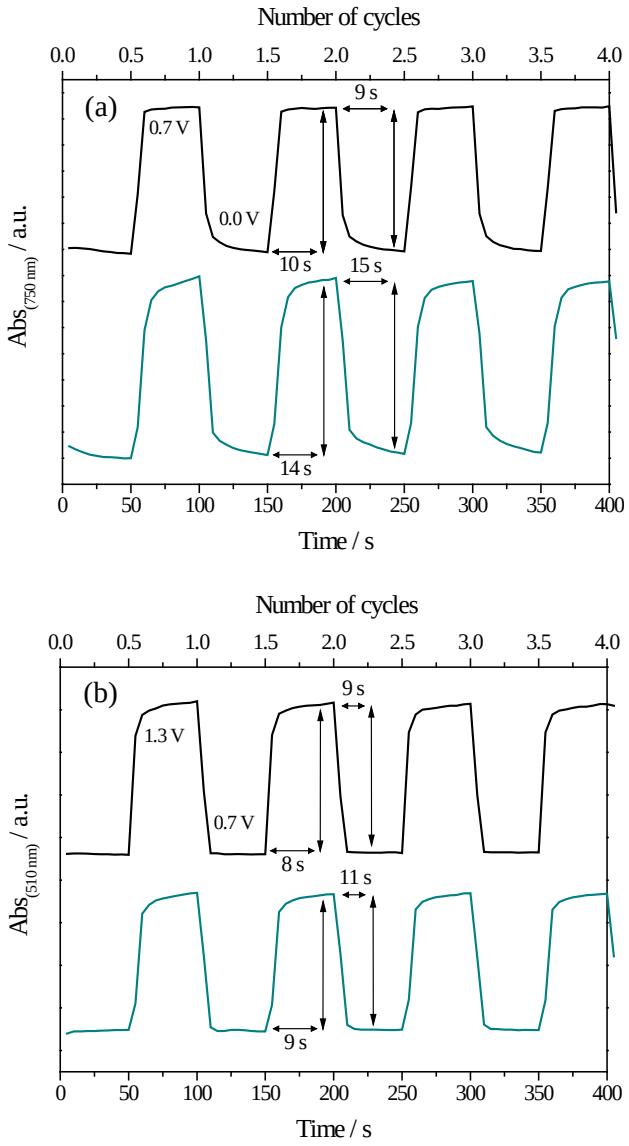


**Figure S6.** Chronoabsorptograms obtained for poly[2] films in $LiClO_4/CH_3CN$ (—) and $LiClO_4$/PC (—), for the colour transitions (a) yellow ↔ green (λ=750 nm) and (b) green ↔ russet (λ=510 nm), with indication of the estimated switching times.

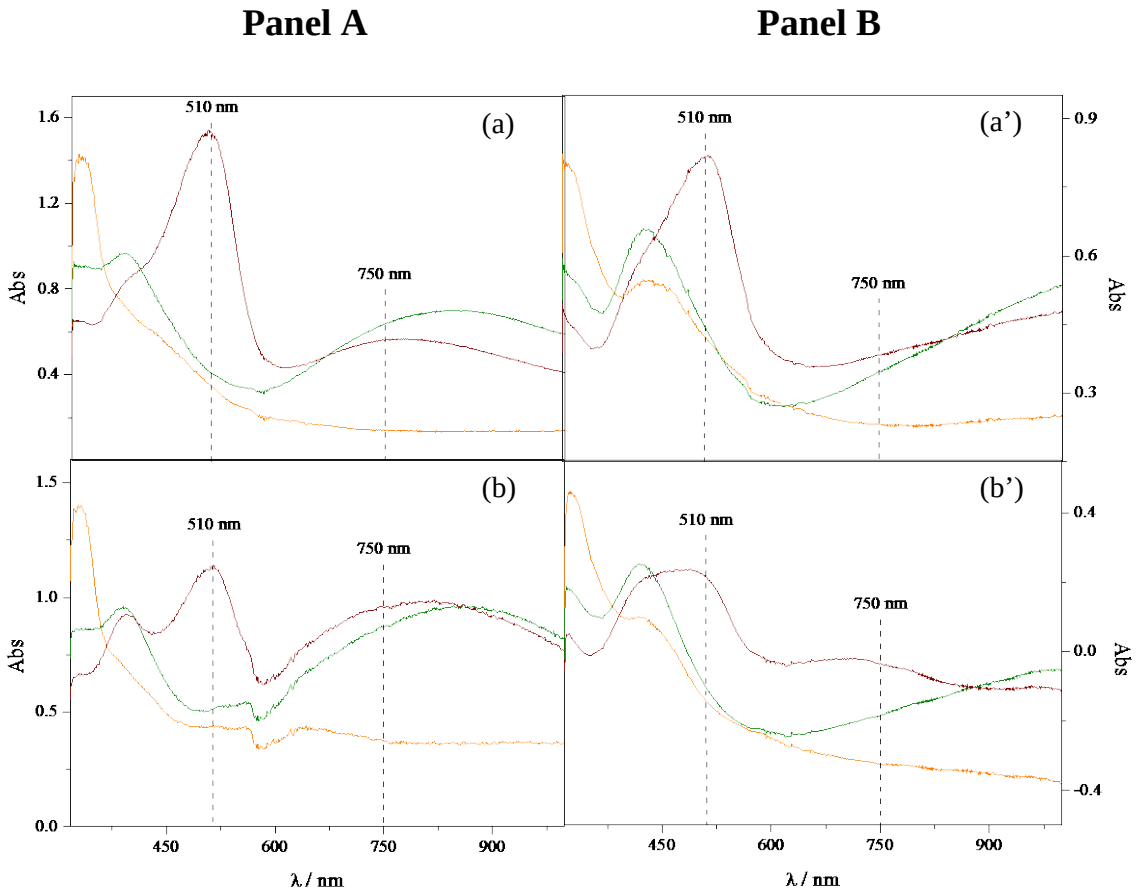


**Figure S7.** UV-Vis spectra of poly[1] (Panel A) and poly[2] (Panel B) films in $LiClO_4/CH_3CN$ (a and a') and $LiClO_4$/PC (b and b') in different oxidation states, corresponding to the colours yellow (0.0 V,—), green (0.7 V,—) and russet (1.3 V,—). The spectra are acquires after applying the indicated potential values during 50 s.

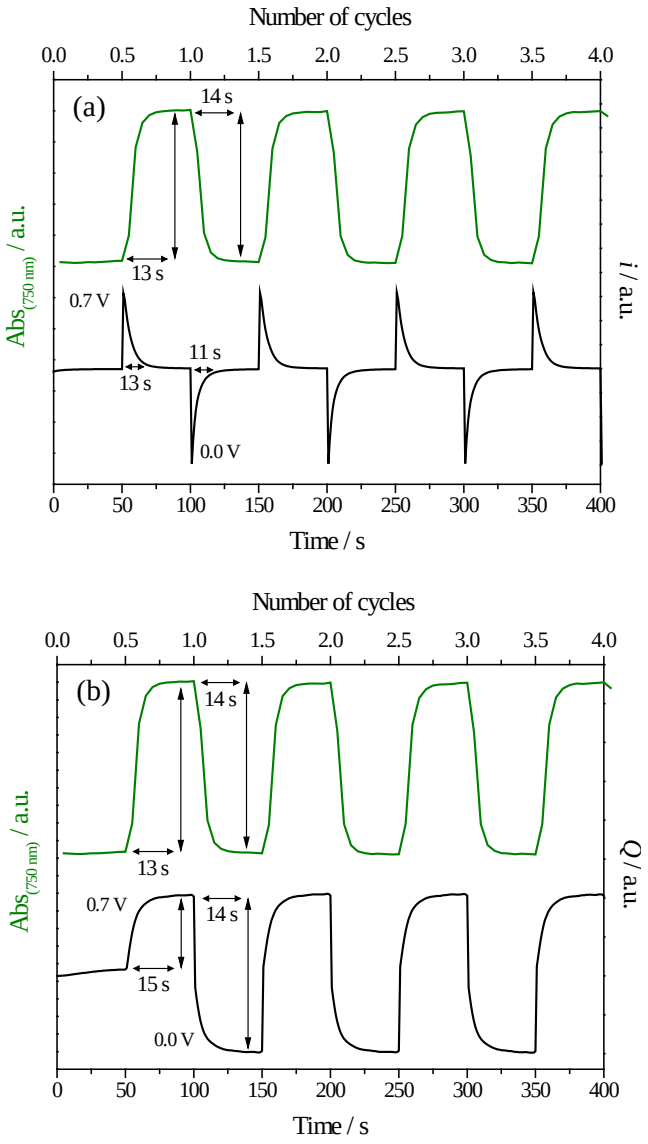


**Figure S8.** Chronoabsorptograms and (a) chronoamperograms or (b) chronocoulograms obtained in simultaneous for poly[1] films in $LiClO_4$/PC, considering the colour transition yellow ↔ green (λ=750 nm); in chronoamperometric study were applied two potential pulses of 50 s by redox cycle, with potential alternating between 0.0 and 0.7 V.

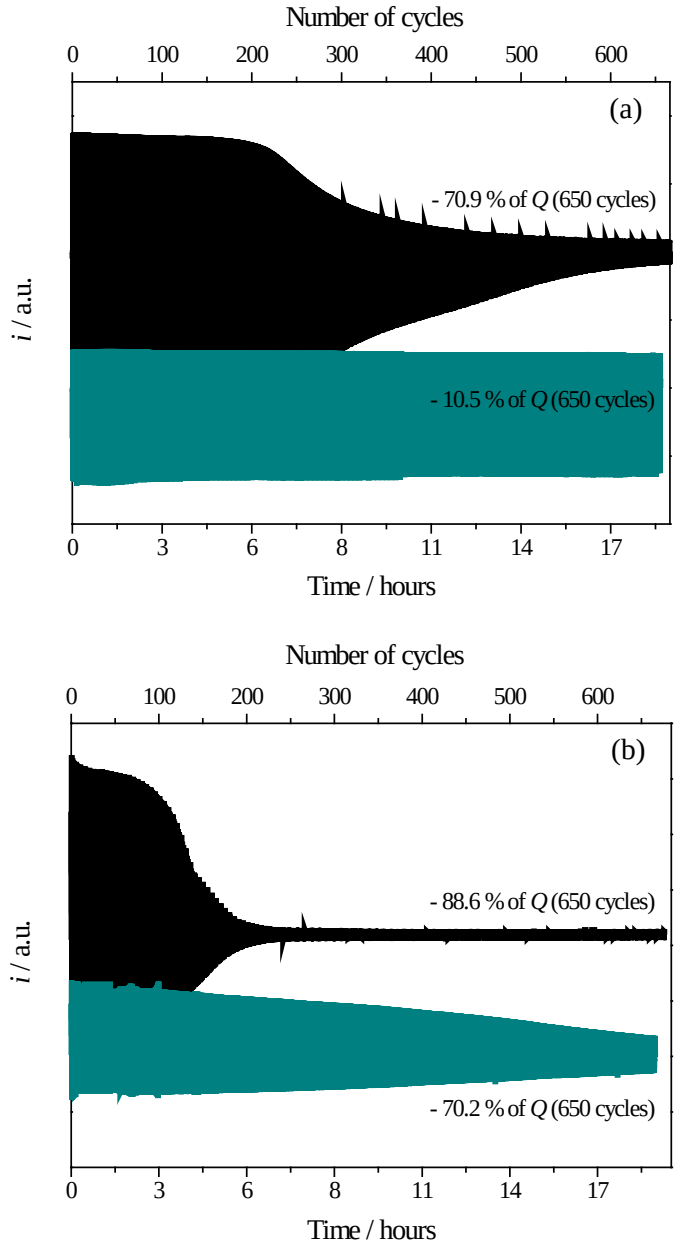


**Figure S9.** Chronoamperograms of poly[2] films in $LiClO_4/CH_3CN$ (—) and $LiClO_4/PC$ (—) for the colour changes (a) yellow-green and (b) green-russet, applying two potential pulses of 50 s by redox cycle, with potential alternating between (a) 0.0 - 0.7 V and (b) 0.7 – 1.15 V.

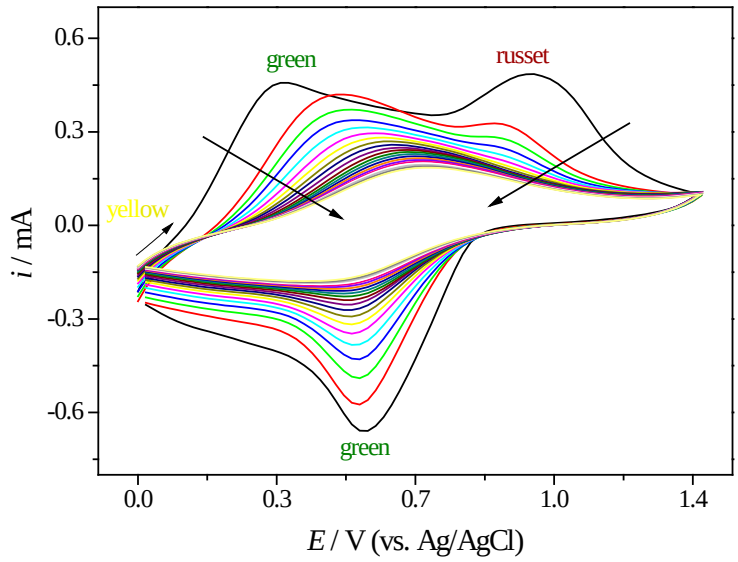


**Figure S10.** Voltammetric responses of poly[1] in $LiClO_4$/PC 0.1 mol $dm^{-3}$, obtained at scan rate of 20 mV $s^{-1}$, during 200 scans.

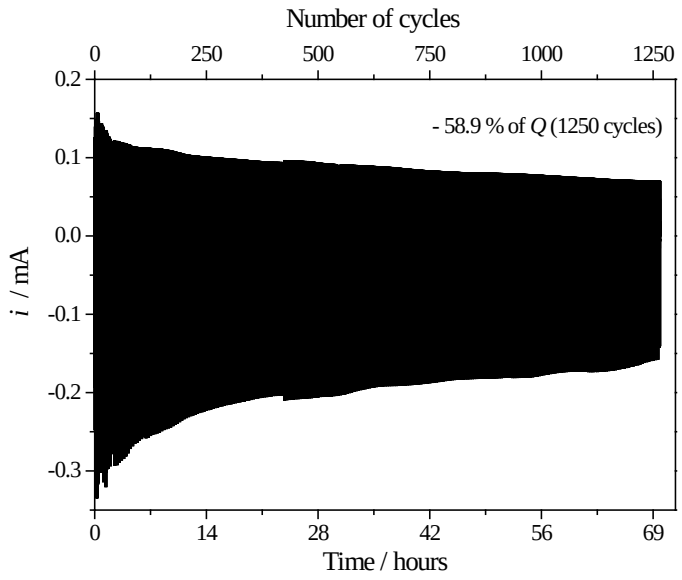


**Figure S11.** Chronoamperograms of the ECD of typology 2, applying two potential pulses of 100 s by redox cycle, with potential alternating between -1.1 (yellow) and -0.25 V (green).